

Gravitational waves from first order electroweak phase transition in models with the $U(1)_X$ gauge symmetry



Toshinori Matsui¹

Collaborators:

Katsuya Hashino^{2,3}, Mitsuru Kakizaki², Shinya Kanemura³, Pyungwon Ko¹

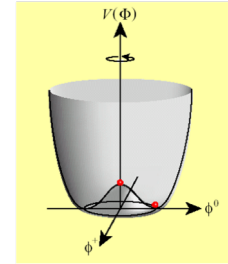
¹KIAS (Korea), ²U. of Toyama (Japan), ³Osaka U. (Japan)

JHEP 1806, 088 (2018) [arXiv:1802.02947]

Physics behind the EW symmetry breaking

- The SM has been established as a low-energy eff. theory by the discovery of the Higgs boson.
- However, we have not understood the structure of the Higgs sector.

$$\mathcal{L}_{\text{SM}}^{\Phi} = |D_{\mu}\Phi|^2 - V_{\text{SM}}(\Phi) - \bar{\psi}_i y_{ij} \psi_j \Phi + \text{h.c.}$$



- The SM has minimal Higgs potential. $V_{\text{SM}}(\Phi) = \mu^2|\Phi|^2 + \frac{\lambda}{2}|\Phi|^4$ $\Phi = \begin{pmatrix} w^+ \\ \frac{1}{\sqrt{2}}(h + iz) \end{pmatrix}$

- Higgs self-couplings have not been measured!

Predictions \rightarrow

$$m_h^2 = \left. \frac{d^2V}{dh^2} \right|_{h \rightarrow v} = \lambda v^2 \quad \lambda_{hhh}^{\text{SM}} \equiv \left. \frac{d^3V}{dh^3} \right|_{h \rightarrow v} = \frac{3m_h^2}{v}$$

- Higgs boson couplings might be deviated from the prediction in the SM.



- On the other hand, new physics is required to solve BSM phenomena.

BSM (such as BAU, DM) might be related to the extended Higgs sector.

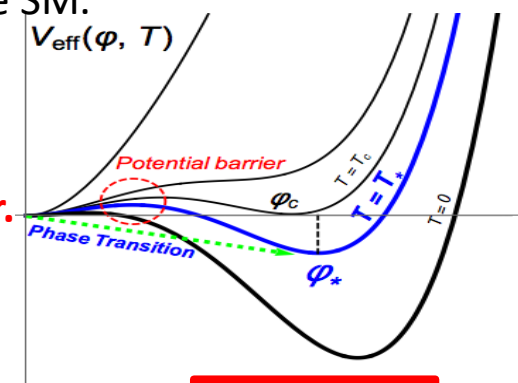
- Exploring the dynamics of EW symmetry breaking is important.

- EW phase transition at finite temperature (1st order? 2nd order?)

- In order to satisfy the 3rd condition of Sakharov's conditions, **strongly 1stOPT** ($\varphi_*/T_* \gtrsim 1$) (sphaleron decoupling criterion) is required in *Electroweak baryogenesis* scenario.

- In the SM with $m_h=125$ GeV, 1st order EW phase transition is not realized.

We investigate detectability of GWs from 1stOPT in dark sector with extended Higgs models.



$$\varphi_*/T_* \gtrsim 1$$

$$\Phi = \begin{pmatrix} w^+ \\ \frac{1}{\sqrt{2}}(v_\Phi + \phi_1 + iz) \end{pmatrix}$$

Higgs portal DM (renormalizable model) with 1stOPT

Singlet scalar DM (5 parameters) $\mathcal{L}_{\text{SSDM}} = -V_0(\Phi, S)$ [1210.4196](#), [1409.0005](#), [1611.02073](#),
[1702.06124](#), [1704.03381](#), ...

$$V_0(\Phi, S) = -\mu_\Phi^2 |\Phi|^2 + \frac{1}{2} \mu_S^2 S^2 + \lambda_\Phi |\Phi|^4 + \frac{1}{4} \lambda_S S^4 + \frac{1}{2} \lambda_{\Phi S} |\Phi|^2 S^2 \quad \langle S \rangle = 0$$

$$m_S^2 = \mu_S^2 + \lambda_{HS} v^2$$

Scalar potential is imposed unbroken Z_2 symmetry.

PT can be caused by thermal loop effect, but excluded by DM direct searches.

Singlet Fermion DM (10 parameters)

$$\mathcal{L}_{\text{SFDM}} = \bar{\psi}(i\not{\partial} - \underline{m_{\psi_0}})\psi - \underline{\lambda S} \bar{\psi}\psi - V_0(\Phi, S) \quad \begin{matrix} 1112.1847, 1209.4163, \\ 1305.3452, 1402.3087, \dots \end{matrix}$$

$$V_0(\Phi, S) = -\mu_\Phi^2 |\Phi|^2 + \lambda_\Phi |\Phi|^4 + \mu_{\Phi S} |\Phi|^2 S + \frac{\lambda_{\Phi S}}{2} |\Phi|^2 S^2 + \mu_S^3 S + \frac{m_S^2}{2} S^2 + \frac{\mu'_S}{3} S^3 + \frac{\lambda_S}{4} S^4 \quad \begin{matrix} S = v_S + \phi_2 \\ m_\psi \equiv m_{\psi_0} + \lambda v_S \end{matrix}$$

Scalar potential is general shape with a real Higgs singlet scalar field (Higgs singlet model; HSM).

PT can be caused by tree level (mixing) effect of the scalar potential. DM contributes as the loop effect.

Vector DM (6 parameters)

$$\mathcal{L}_{\text{VDM}} = -\frac{1}{4} X_{\mu\nu} X^{\mu\nu} + |D_\mu S|^2 - V_0(\Phi, S) \quad 1212.2131, 1412.3823, \dots$$

$$V_0(\Phi, S) = -\mu_\Phi^2 |\Phi|^2 - \mu_S^2 |S|^2 + \lambda_\Phi |\Phi|^4 + \lambda_S |S|^4 + \lambda_{\Phi S} |\Phi|^2 |S|^2 \quad S = \frac{1}{\sqrt{2}}(v_S + \phi_2 + ix)$$

$$D_\mu S = (\partial_\mu + i \underline{g_X} Q_S X_\mu) S \longrightarrow m_X = g_X |Q_S| v_S$$

Scalar potential is a case for the spontaneously broken Z_2 symmetry in HSM.

U(1)_X model

▪ U(1)_X gauge field (dark photon) X_μ^0 & complex scalar (dark Higgs) S with U(1)_X-charge $Q_S=1$

▪ Lagrangian: $\mathcal{L} = -\frac{1}{4}X_{\mu\nu}X^{\mu\nu} - \frac{\epsilon}{2}X_{\mu\nu}B^{\mu\nu} + |D_\mu S|^2 - V_0(\Phi, S)$ [B. Holdom, PLB166, 196 (1986)]

$$V_0(\Phi, S) = -\mu_\Phi^2|\Phi|^2 - \mu_S^2|S|^2 + \lambda_\Phi|\Phi|^4 + \lambda_S|S|^4 + \lambda_{\Phi S}|\Phi|^2|S|^2$$

- U(1)_X gauge symmetry is spontaneously broken by nonzero VEV of S : Dark Higgs mechanism

$$\Phi = \begin{pmatrix} w^+ \\ \frac{1}{\sqrt{2}}(\underline{v}_\Phi + \phi_\Phi + iz^0) \end{pmatrix}, \quad S = \frac{1}{\sqrt{2}}(\underline{v}_S + \phi_S + ix^0) \quad D_\mu S = (\partial_\mu + ig_X Q_S X_\mu)S \rightarrow m_X \equiv g_X |Q_S| v_S$$

- Fields mixing: $(\phi_\Phi, \phi_S) \rightarrow (\underline{h}, \underline{H})$ with the mixing angle θ

▪ Parameters ($m_h=125$ GeV, $v_\Phi=246$ GeV; $\underline{m}_H, \theta; \underline{m}_X, \underline{g}_X; \epsilon$)

▪ A case for nonzero ϵ

- The parameter space (m_X, ϵ) is constrained by various experiments of **dark photon search**.

- **We investigate the complementarity of dark photon searches and GW observations.**

[Addazi and Marciano, 1703.03248 (CPC)]

▪ An optional case for $\epsilon \rightarrow 0$

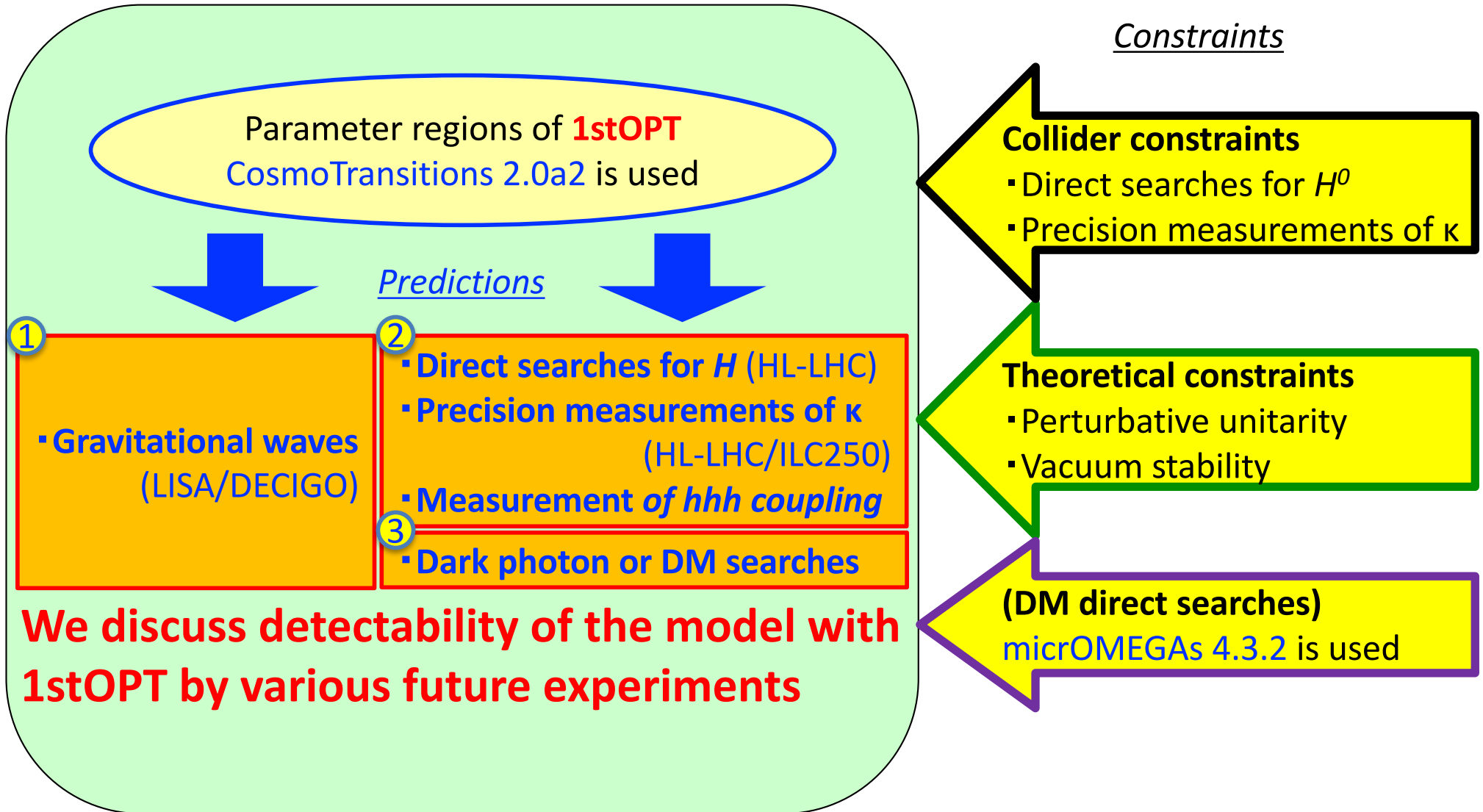
- X_μ^0 boson can be a DM candidate if we assume it to be odd under the Z_2 sym. (**Vector DM**)

[cf. Baek, Ko, Park, Senaha, 1212.2131 (JHEP)]

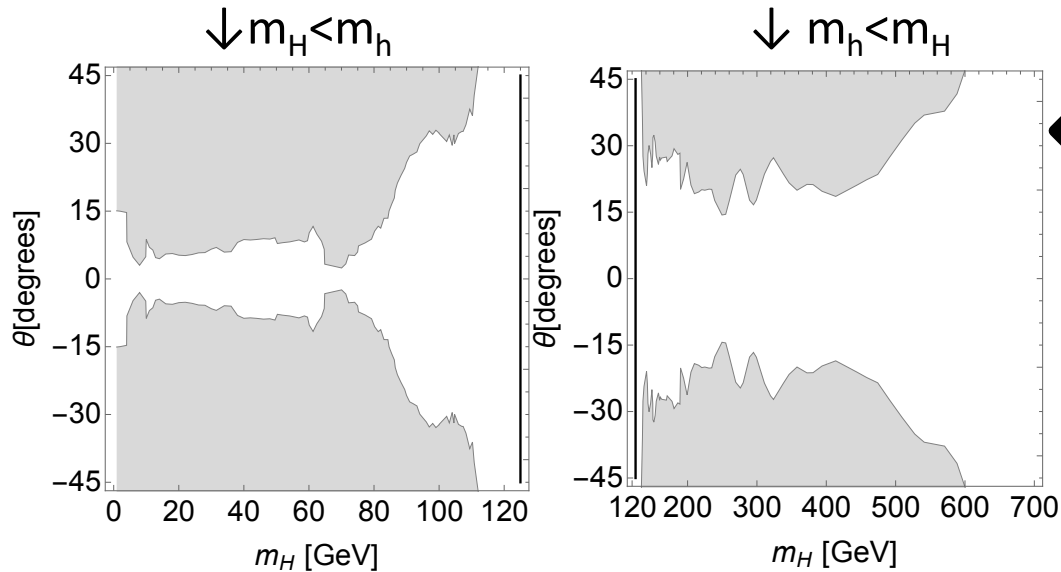
- The Z_2 symmetry removes the kinetic mixing term, making X_μ^0 stable; $\epsilon \rightarrow 0$ limit.

- **We consider current DM constraints as a scenario.**

Detectability of 1stOPT in $U(1)_X$ model



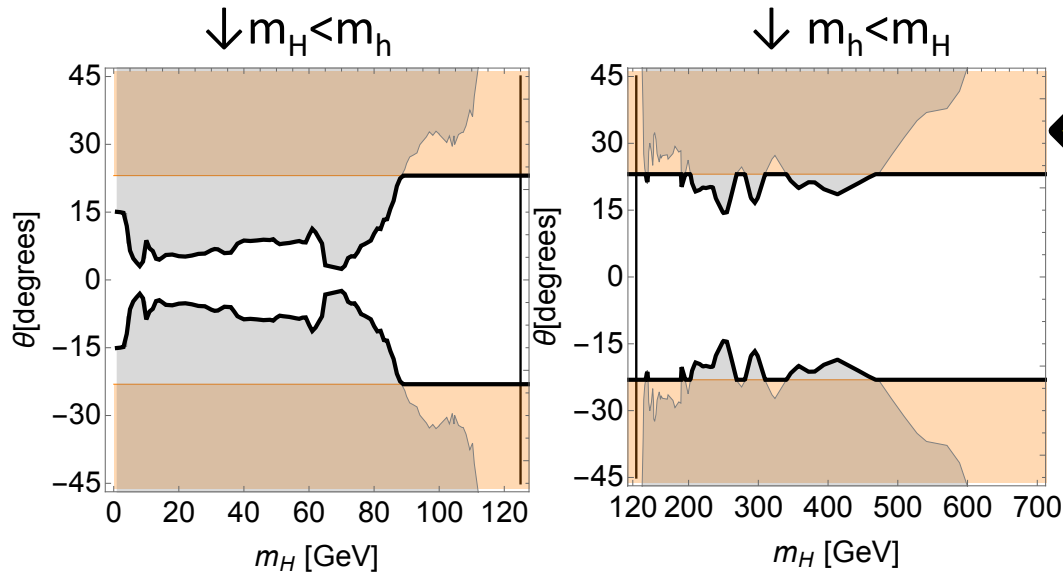
Numerical result on (m_H, θ) plane



Collider constraints

- Direct searches for H @LEP&LHC Run-II (2σ)
[Robens, Stefaniak, 1501.02234 (EPJ); 1601.07880 (EPJ)]

Numerical result on (m_H, θ) plane



Collider constraints

- Direct searches for H @ LEP&LHC Run-II (2σ)
[Robens, Stefaniak, 1501.02234 (EPJ); 1601.07880 (EPJ)]

- Interactions @ LHC Run-I results (1σ)
[ATLAS and CMS, ATLAS-CONF-2015-044]

$$\kappa_Z = 1.03^{+0.11}_{-0.11} \quad \kappa_W = 0.91^{+0.10}_{-0.10} \quad \Rightarrow \quad |\theta| \leq 23.1^\circ$$

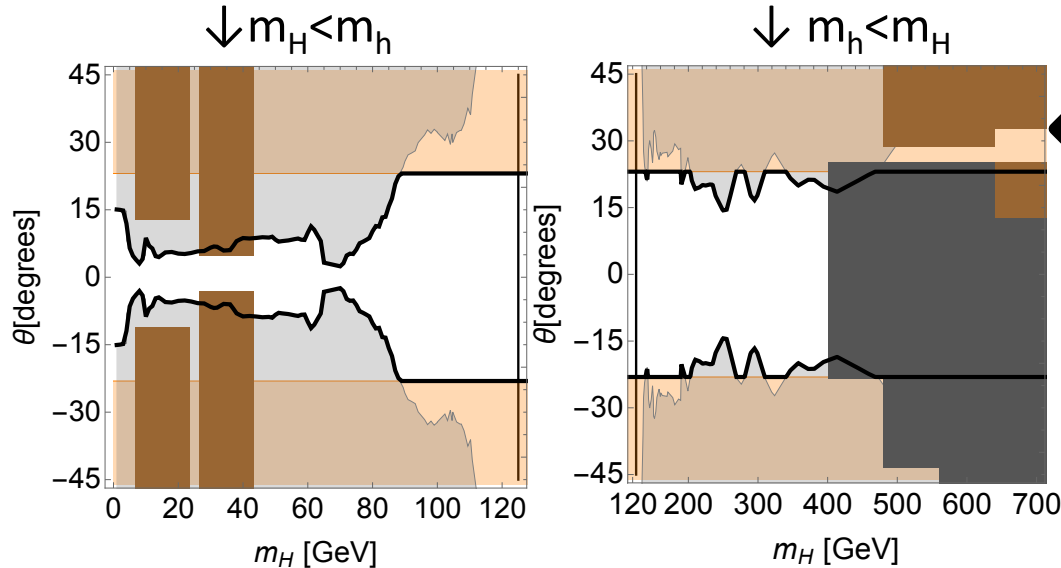
Interactions (hVV, hff) [Prediction]

$$\kappa \equiv \frac{g_{hVV}}{g_{hVV}^{\text{SM}}} = \frac{g_{hff}}{g_{hff}^{\text{SM}}} = \cos \theta$$

Numerical result on (m_H, θ) plane

$m_\chi=200\text{GeV}, g_\chi=2$ ($v_s=100\text{GeV}$) as an example

Hashino, Kakizaki, Kanemura, Ko, TM, 1802.02947 (JHEP)



Collider constraints

- Direct searches for H @ LEP&LHC Run-II (2σ)
[Robens, Stefaniak, 1501.02234 (EPJ); 1601.07880 (EPJ)]
- Interactions @ LHC Run-I results (1σ)
[ATLAS and CMS, ATLAS-CONF-2015-044]

$$\kappa_Z = 1.03^{+0.11}_{-0.11} \quad \kappa_W = 0.91^{+0.10}_{-0.10} \quad \Rightarrow \quad |\theta| \leq 23.1^\circ$$

Interactions (hVV, hff) [Prediction]

$$\kappa \equiv \frac{g_{hVV}}{g_{hVV}^{\text{SM}}} = \frac{g_{hff}}{g_{hff}^{\text{SM}}} = \cos \theta$$

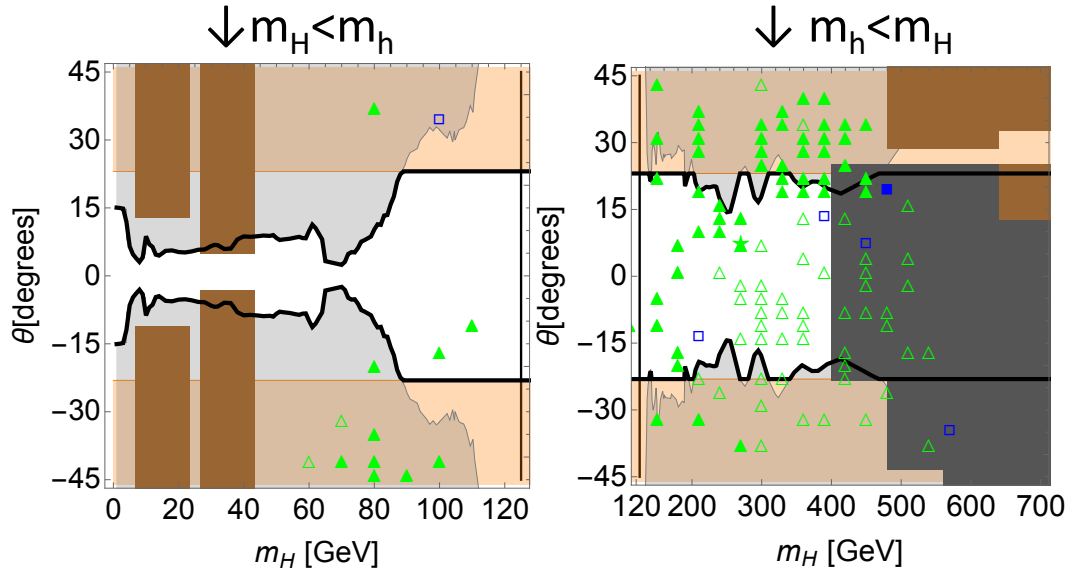
Theoretical constraints

- Perturbative unitarity
- Vacuum stability

Numerical result on (m_H, θ) plane

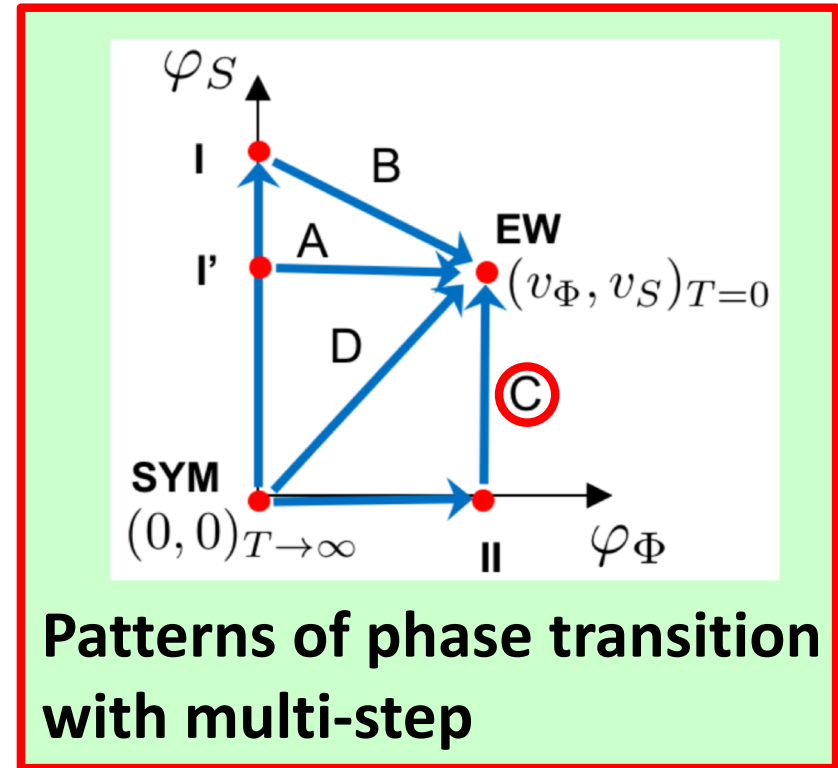
$m_X=200\text{GeV}, g_X=2$ ($v_S=100\text{GeV}$) as an example

Hashino, Kakizaki, Kanemura, Ko, TM, 1802.02947 (JHEP)



Parameter regions of **1stOPT**

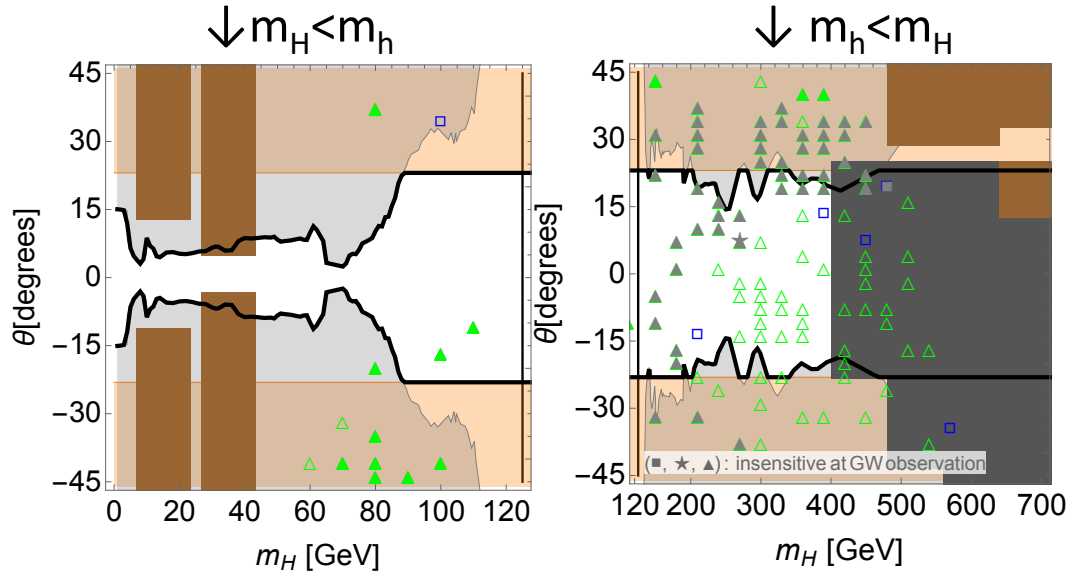
■	one-step PT (1st order)
□	one-step PT (2nd order)
★	two-step PT (1st order → 1st order)
▲	two-step PT (2nd order → 1st order)
△	two-step PT (1st order → 2nd order)



Numerical result on (m_H, θ) plane

$m_X=200\text{GeV}, g_X=2$ ($v_s=100\text{GeV}$) as an example

Hashino, Kakizaki, Kanemura, Ko, TM, 1802.02947 (JHEP)

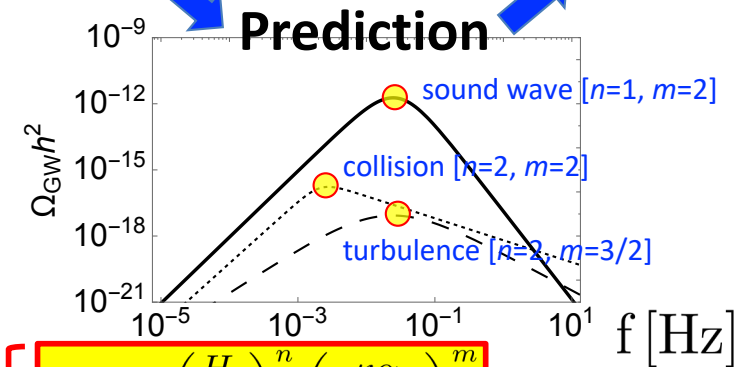
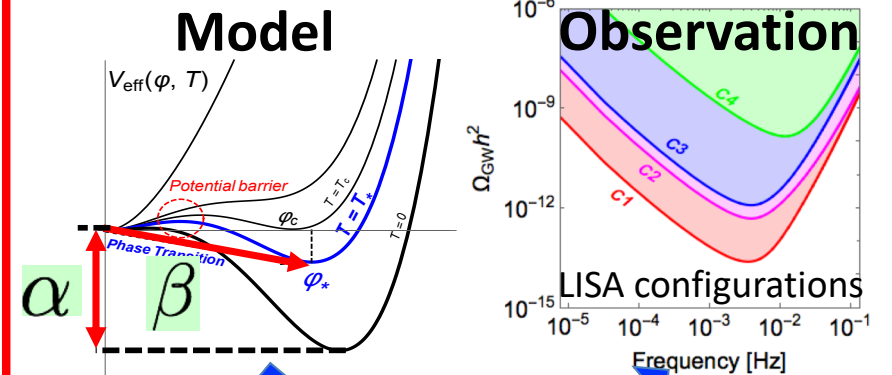


Parameter regions of **1stOPT**

① **Gravitational waves (LISA and DECIGO)**

■	one-step PT (1st order)
□	one-step PT (2nd order)
★	two-step PT (1st order → 1st order)
▲	two-step PT (2nd order → 1st order)
△	two-step PT (1st order → 2nd order)
(■, ★, ▲) in (m_H, θ)	<u>insensitive at GW observation</u>

$\alpha \sim$ Normalized difference of the potential minima
 $\beta^{-1} \sim$ Transition time \propto Bubble size

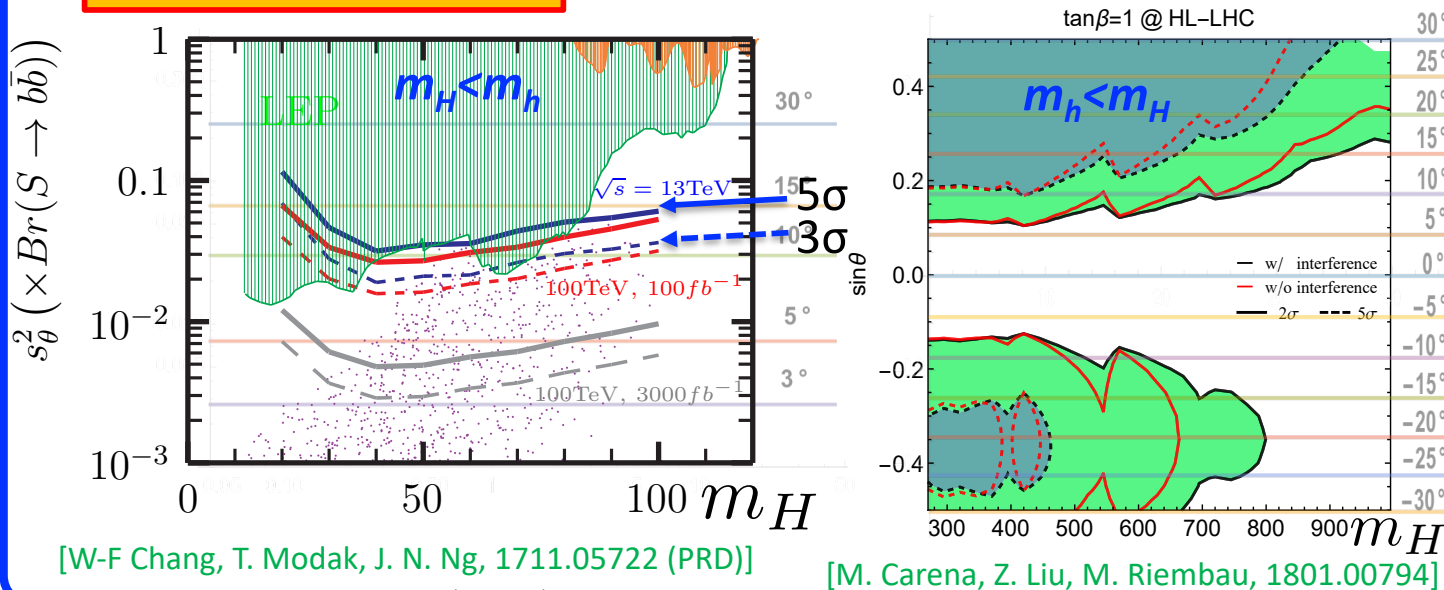


$$\Omega_{\text{GW}} \propto \left(\frac{H_t}{\beta}\right)^n \left(\frac{\kappa\alpha}{1+\alpha}\right)^m$$

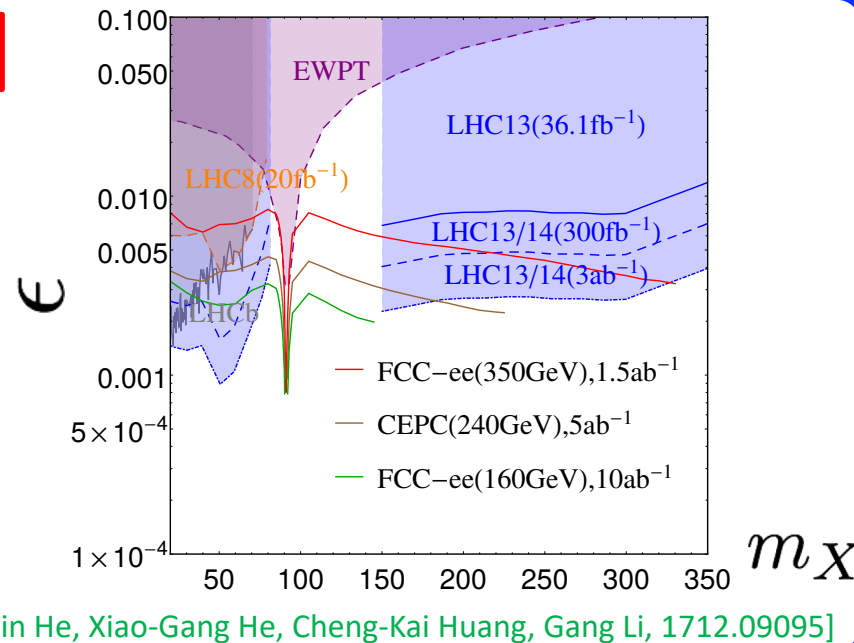
$$f_0 \simeq 10^{-(3-1)} \text{Hz} \frac{T_t}{100\text{GeV}} \frac{\beta/H_t}{10^{2-4}}$$

C. Caprini et al., 1512.06239 (JCAP)

2 Direct searches for H @HL-LHC (13TeV, 3ab⁻¹), 100TeV-pp (0.1/3ab⁻¹)



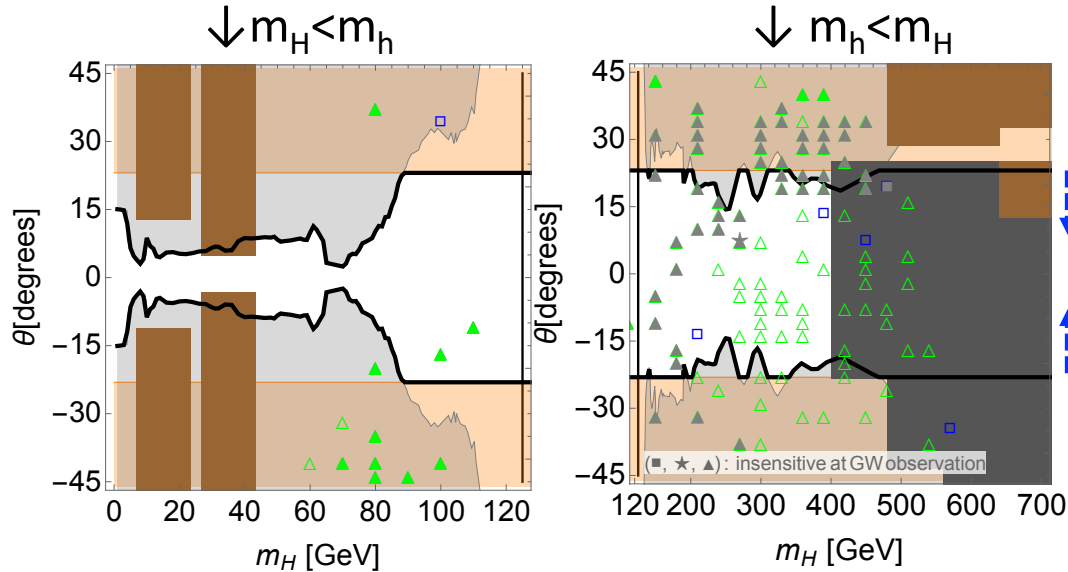
3 Dark photon searches



Numerical result on (m_H, θ) plane

$m_x=200\text{GeV}, g_x=2$ ($v_s=100\text{GeV}$) as an example

Hashino, Kakizaki, Kanemura, Ko, TM, 1802.02947 (JHEP)



Interactions (hVV, hff) [Prediction]

$$\kappa \equiv \frac{g_{hVV}^{\text{SM}}}{g_{hVV}} = \frac{g_{hff}^{\text{SM}}}{g_{hff}} = \cos \theta$$

Indirect searches

Precision measurements of κ

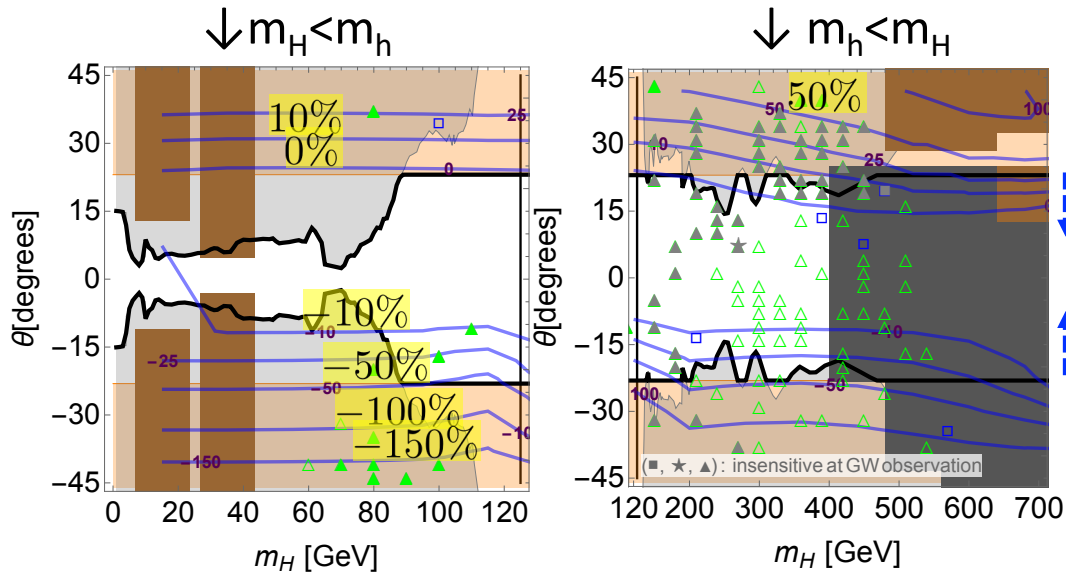
“Expected accuracy of κ ”

- $\Delta\kappa_V: 2\% @ \text{HL-LHC } 14\text{TeV } 3\text{ab}^{-1}$
[CMS, 1307.7135]
- $\Delta\kappa_{Z(W)}: 0.38 (1.8)\% @ \text{ILC } 250\text{GeV } 2\text{ab}^{-1}$
[Fujii et al., 1710.07621]

Numerical result on (m_H, θ) plane

$m_X=200\text{GeV}, g_X=2$ ($v_S=100\text{GeV}$) as an example

Hashino, Kakizaki, Kanemura, Ko, TM, 1802.02947 (JHEP)



Interactions (hVV, hff) [Prediction]

$$\kappa \equiv \frac{g_{hVV}}{g_{hVV}^{\text{SM}}} = \frac{g_{hff}}{g_{hff}^{\text{SM}}} = \cos \theta$$

Indirect searches

Precision measurements of κ

“Expected accuracy of κ ”

- $\Delta\kappa_V: 2\% @ \text{HL-LHC } 14\text{TeV } 3\text{ab}^{-1}$
[CMS, 1307.7135]
- $\Delta\kappa_{Z(W)}: 0.38$ (1.8)% @ ILC 250GeV 2ab⁻¹
[Fujii et al., 1710.07621]

Measurement of hhh coupling

$$\frac{\Delta\lambda_{hhh}}{\lambda_{hhh}^{\text{SM}}} \equiv \frac{\lambda_{hhh} - \lambda_{hhh}^{\text{SM}}}{\lambda_{hhh}^{\text{SM}}}$$

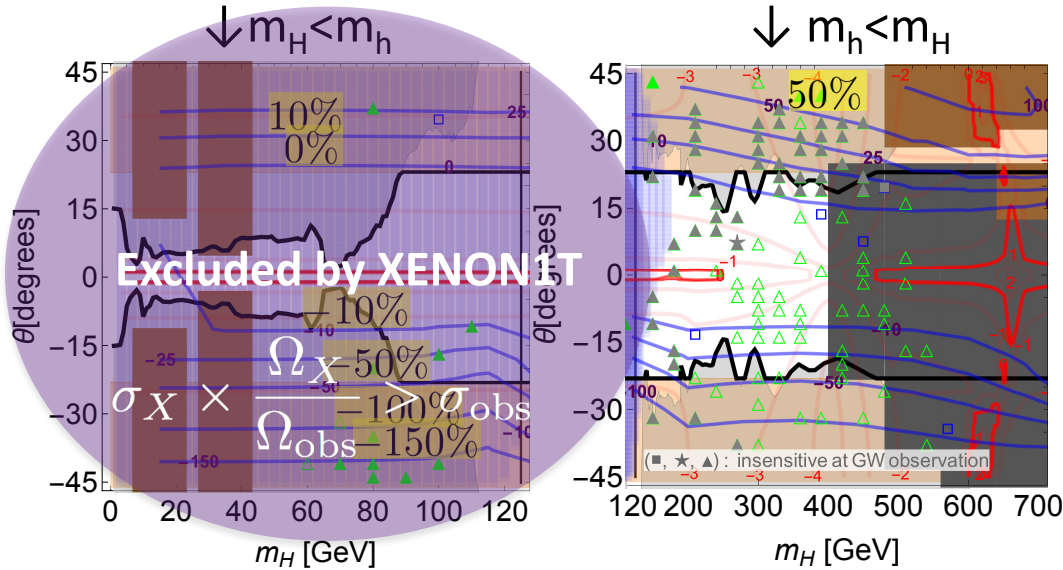
“Expected accuracy”

- $-0.8 \lesssim \Delta\lambda_{hhh}/\lambda_{hhh}^{\text{SM}} \lesssim 7.7 @ \text{HL-LHC } 14\text{TeV } 3\text{ab}^{-1}$
[ATL-PHYS-PUB-2017-001]
- $\Delta\lambda_{hhh}: 16$ (10)% @ ILC 1TeV 2 (5)ab⁻¹
[Fujii et al., 1506.05992]

Numerical result on (m_H, θ) plane

$m_X=200\text{GeV}, g_X=2$ ($v_s=100\text{GeV}$) as an example

Hashino, Kakizaki, Kanemura, Ko, TM, 1802.02947 (JHEP)



A case for X^0 -boson as vector DM w/ Z_2 (constraint for $\epsilon \rightarrow 0$)

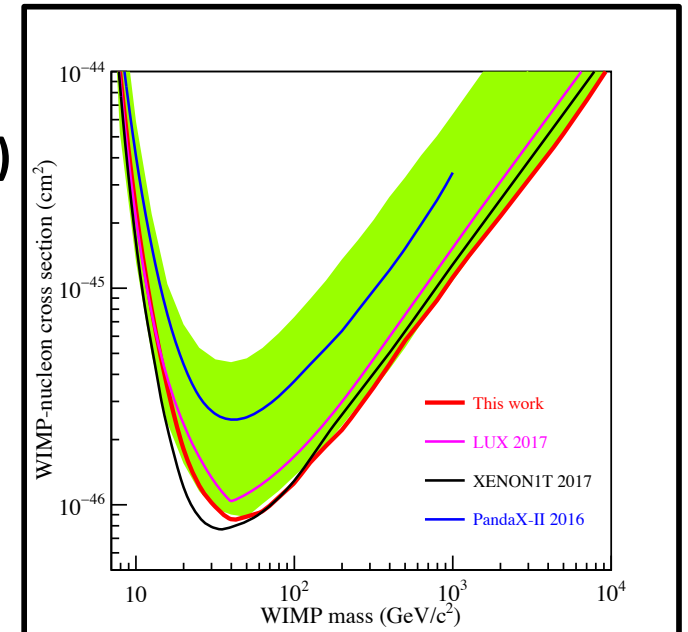
DM searches

• Relic abundance of DM

$\Omega_{\text{obs}} h^2 = 0.1199 \pm 0.0027 \rightarrow$ contours of $\log_{10} (\Omega_X / \Omega_{\text{obs}})$
[Planck Collaboration, 1502.01589 (Astron. Astrophys.)]

• DM direct detection bound

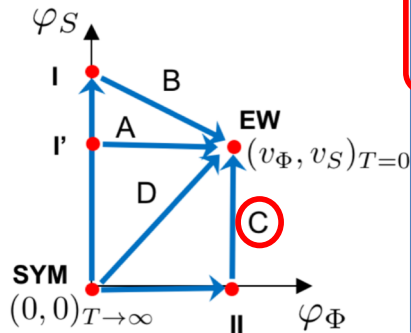
[XENON Collaboration, 1705.06655 (PRL)]



Summary of numerical results

Hashino, Kakizaki, Kanemura, Ko, TM, 1802.02947 (JHEP)

(*1) Patterns of phase transition

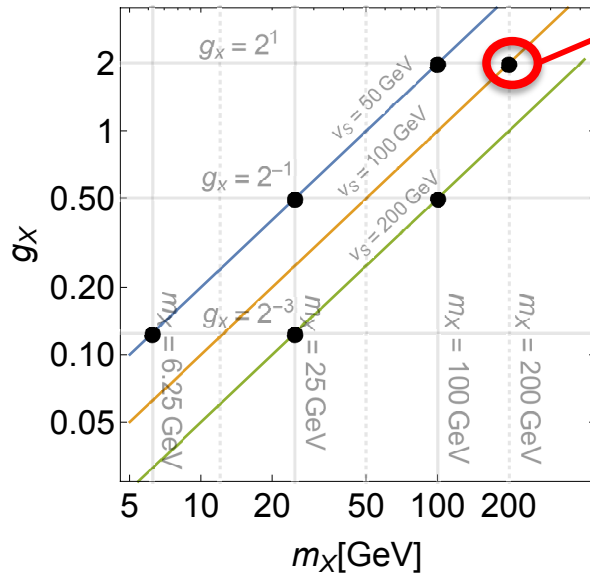


$(m_X [\text{GeV}], g_X)_{v_s}$	Fig.	#	PT	GW	DM
(200, 2) _{100GeV}	3, 4	1	C	●	excluded by XENON1T
		2	C	△	●
		3	D	△	△
(100, 2) _{50GeV}	5	4	C	○	excluded by XENON1T
(100, 0.5) _{200GeV}	6	5	C	○	excluded by XENON1T
		6	D	excluded by collider	excluded by XENON1T
(25, 0.5) _{50GeV}	7	7	C	○	excluded by XENON1T
(25, 0.125) _{200GeV}	8	8	C	excluded by collider	excluded by XENON1T
(6.25, 0.125) _{50GeV}	9	9	D	excluded by collider	excluded by XENON1T

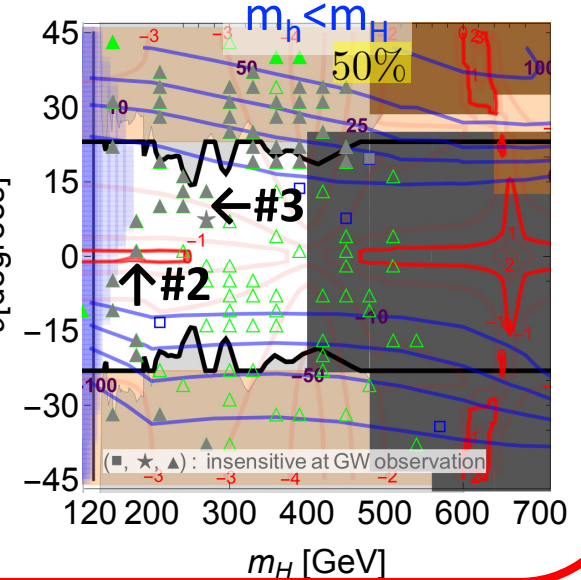
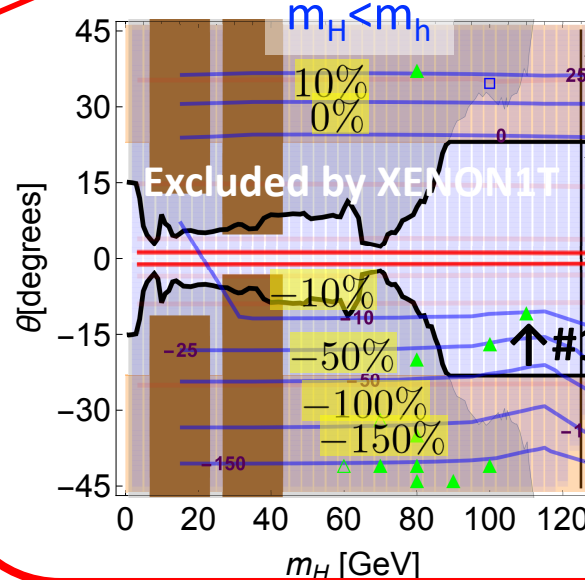
(*2) Detectability of “Gravitational wave” “DM for imposing Z_2 ”

△(GW): signal is too weak
△(DM): $\log_{10}(\Omega_X/\Omega_{\text{obs}}) < 1$

Six benchmark points



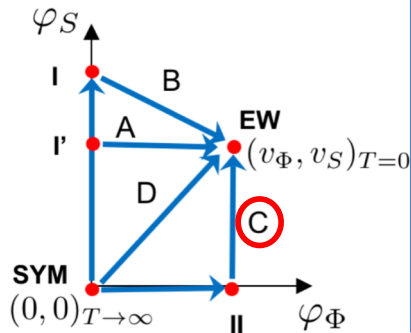
$m_X=200\text{GeV}, g_X=2$ ($v_s=100\text{GeV}$)



Detectable GW signal is preferred for $m_X \gtrsim 25\text{GeV}$ with $g_X \gtrsim 0.5$

Hashino, Kakizaki, Kanemura, Ko, TM, 1802.02947 (JHEP)

(*1) Patterns of phase transition

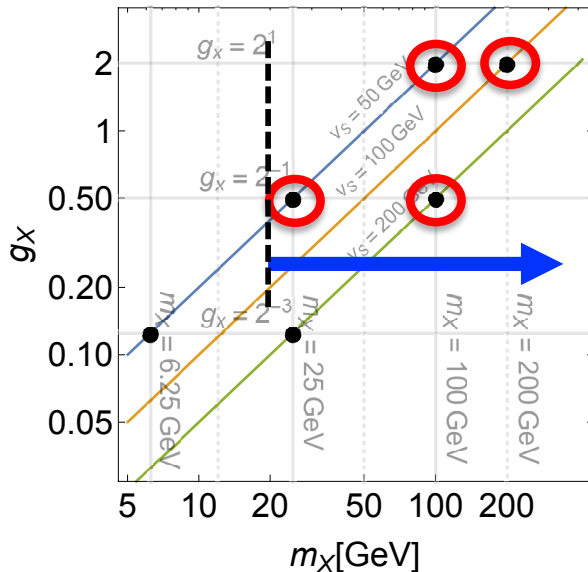


$(m_X[\text{GeV}], g_X)_{v_s}$	Fig.	#	PT	GW	DM
(200, 2) _{100GeV}	3, 4	1	C	●	excluded by XENON1T
		2	C	△	○
		3	D	△	△
(100, 2) _{50GeV}	5	4	C	●	excluded by XENON1T
(100, 0.5) _{200GeV}	6	5	C	●	excluded by XENON1T
		6	D	excluded by collider	excluded by XENON1T
(25, 0.5) _{50GeV}	7	7	C	●	excluded by XENON1T
(25, 0.125) _{200GeV}	8	8	C	excluded by collider	excluded by XENON1T
(6.25, 0.125) _{50GeV}	9	9	D	excluded by collider	excluded by XENON1T

(*2) Detectability of [“Gravitational wave” “DM for imposing Z_2 ”]

△(GW): signal is too weak
△(DM): $\log_{10}(\Omega_X/\Omega_{\text{obs}}) < 1$

Six benchmark points



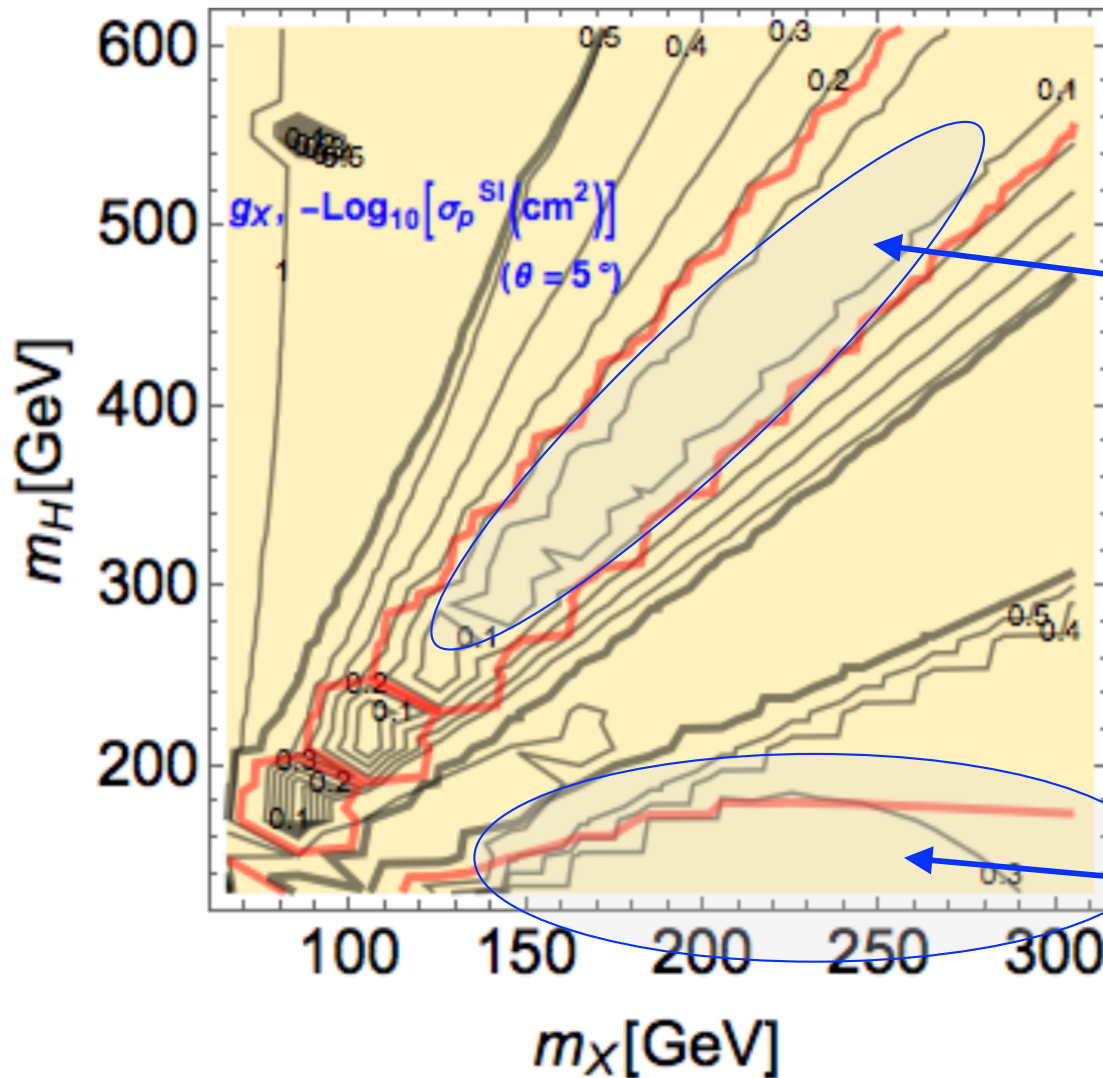
We expect the complementarity of dark photon searches (or DM) searches with GW observations!

Conclusions

- We have investigated models with $U(1)_X$ gauge symmetry.
 - Mass of a dark photon (X_μ), which can be vector DM by imposing Z_2 , is generated by spontaneous breaking of a dark Higgs field (S).
- We have explored comprehensively the patterns of PT and the detectability of GWs from 1stOPT as well as various collider and theoretical bounds.
- **We expect the model with 1stOPT will be tested by the complementarity of GW observations and (in)direct searches for 2nd Higgs boson and dark photon (or DM).**
 - We have found that GW signals are detectable only for larger dark photon mass region ($m_X \gtrsim 25$ GeV with $g_X \gtrsim 0.5$).

Back Up

Vector DM model

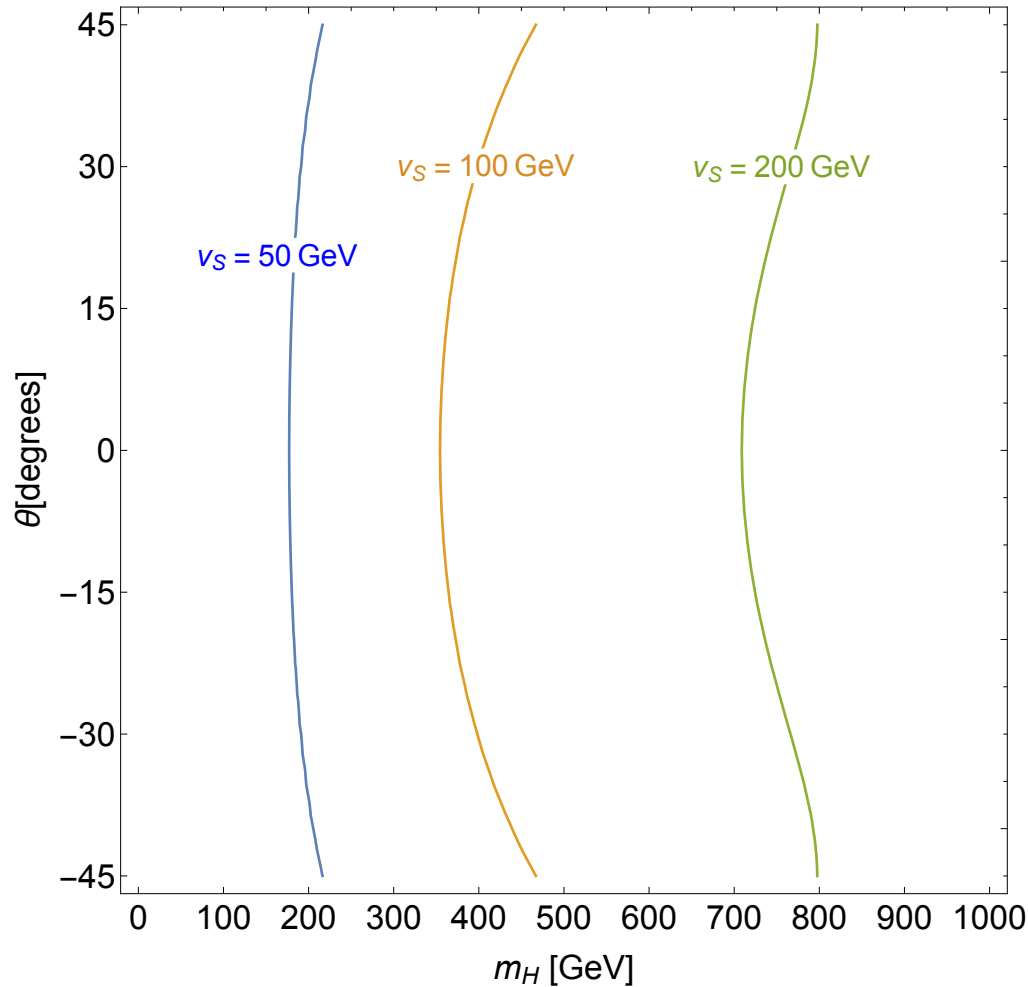


$$\sigma_X = \frac{\cos^2 \theta \sin^2 \theta \mu^2}{\pi} \left(\frac{m_X m_p f_p}{v v_s} \left(\frac{1}{m_h^2} - \frac{1}{m_H^2} \right) \right)^2$$

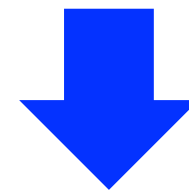
A resonance
at $m_X = m_H/2$

$XX \rightarrow hh, HH, hH$ begin
to open for $m_X > m_h, m_H$

[Theoretical constraint] Perturbative unitarity



The absolute values of eigenvalues of S-wave scattering amplitudes for the longitudinal components of weak gauge bosons and the scalar bosons should be smaller than 1/2

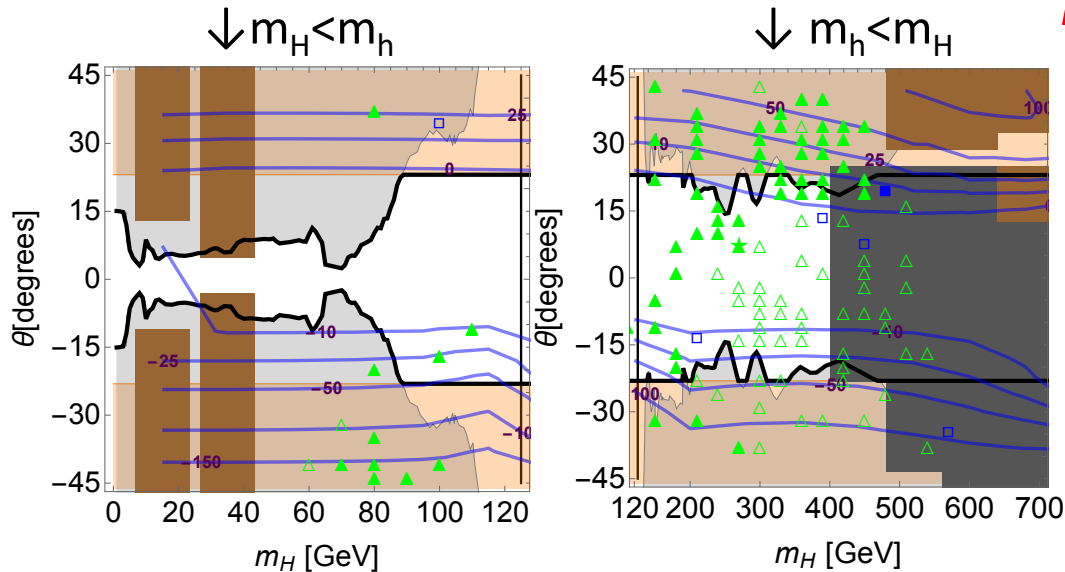


$$|\lambda_\Phi| < 4\pi, |\lambda_S| < 4\pi, |\lambda_{\Phi S}| < 8\pi, 3\lambda_\Phi + 2\lambda_S + \sqrt{(3\lambda_\Phi - 2\lambda_S)^2 + 2\lambda_{\Phi S}^2} < 8\pi$$

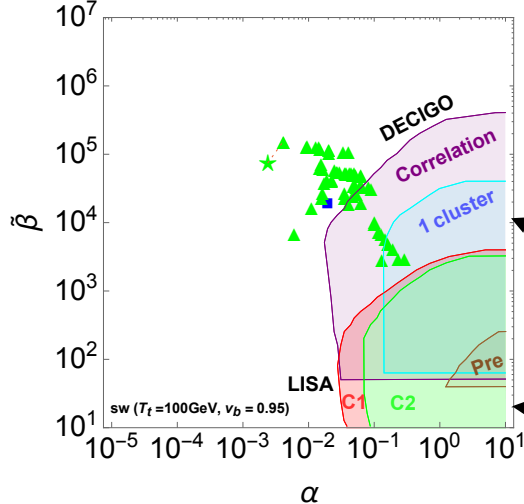
A numerical result on (m_H, θ) by fixing (m_X, g_X)

Hashino, Kakizaki, Kanemura, Ko, TM, 1802.02947

$m_X=200\text{GeV}, g_X=2$ ($v_S=100\text{GeV}$) as an example



Categories	Symbols	Legends
Theory	[Brown shaded box]	excluded by perturbative unitarity
		excluded by vacuum stability
	[Blue line]	contours of $\Delta\lambda_{hhh}/\lambda_{hhh}^{\text{SM}}$ (%)
		combined exclusion limit ([Orange shaded box] + [Grey shaded box])
Collider	[Orange shaded box]	constraint by the κ_Z measurement (see Eq. (4.3))
	[Grey shaded box]	constraint by the direct searches for the H -boson (see Ref. [119])
	[Blue shaded box]	one-step PT (1st order)
	[Blue square]	one-step PT (2nd order)
	[Green star]	two-step PT (1st order \rightarrow 1st order)
	[Green triangle]	two-step PT (2nd order \rightarrow 1st order)
	[Green triangle]	two-step PT (1st order \rightarrow 2nd order)
GW	[Pink shaded box]	DECIGO (Correlation)
	[Light blue shaded box]	DECIGO (1 cluster)
	[Light brown shaded box]	DECIGO (Pre)
	[Red shaded box]	LISA (C1)
	[Green shaded box]	LISA (C2)



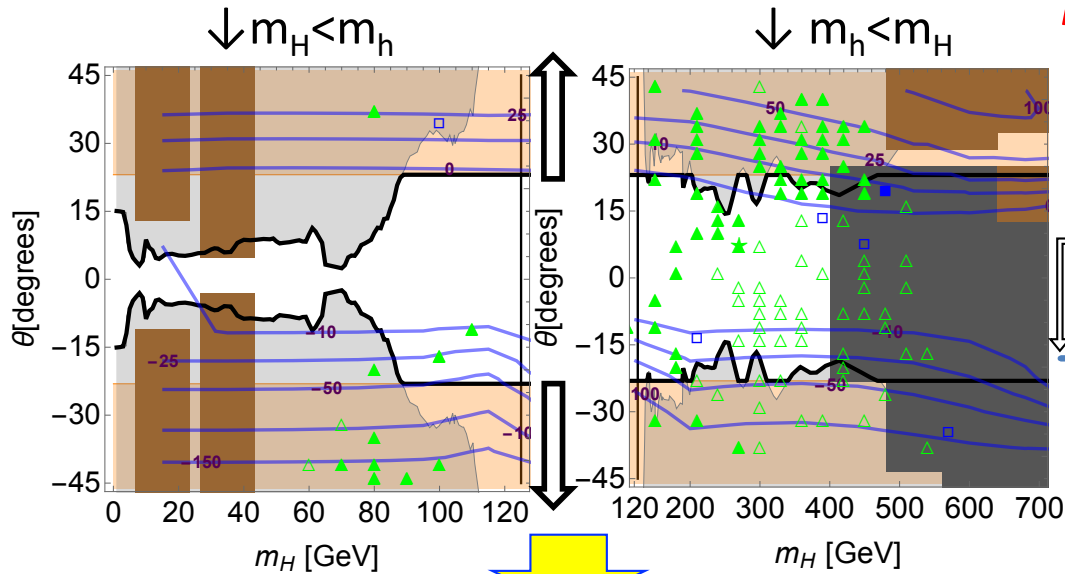
Sensitivities

- DECIGO [S.Kawamura, et al., *Class. Quant. Grav.* **28**, 094011 (2011)]
- eLISA [C.Caprini et al., arXiv:1512.06239 (JCAP)]

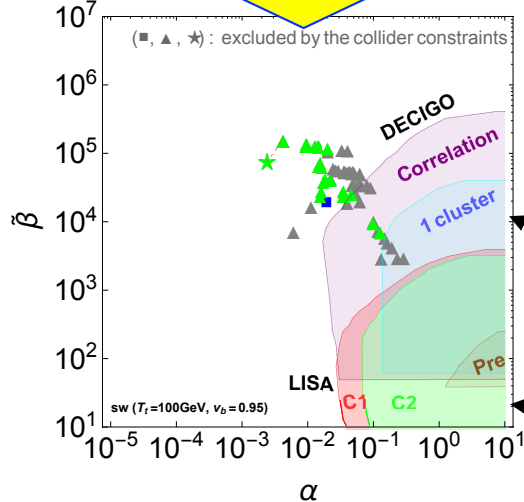
A numerical result on (m_H, θ) by fixing (m_X, g_X)

Hashino, Kakizaki, Kanemura, Ko, TM, 1802.02947

$m_X=200\text{GeV}, g_X=2$ ($v_S=100\text{GeV}$) as an example



Categories	Symbols	Legends
Theory	[Solid black bar]	excluded by perturbative unitarity
		excluded by vacuum stability
	[Blue line]	contours of $\Delta\lambda_{hhh}/\lambda_{hhh}^{\text{SM}}$ (%)
		constraint by the κ_Z measurement (see Eq. (4.3))
Collider	[Orange bar]	constraint by the direct searches for the H -boson (see Ref. [119])
	[Grey bar]	combined exclusion limit ([Orange bar] + [Grey bar])
	[Black line]	
PT	[Blue square]	one-step PT (1st order)
	[Blue square]	one-step PT (2nd order)
	[Green star]	two-step PT (1st order \rightarrow 1st order)
	[Green triangle]	two-step PT (2nd order \rightarrow 1st order)
	[Green triangle]	two-step PT (1st order \rightarrow 2nd order)
GW	[Pink bar]	DECIGO (Correlation)
	[Light blue bar]	DECIGO (1 cluster)
	[Light orange bar]	DECIGO (Pre)
	[Red bar]	LISA (C1)
	[Green bar]	LISA (C2)



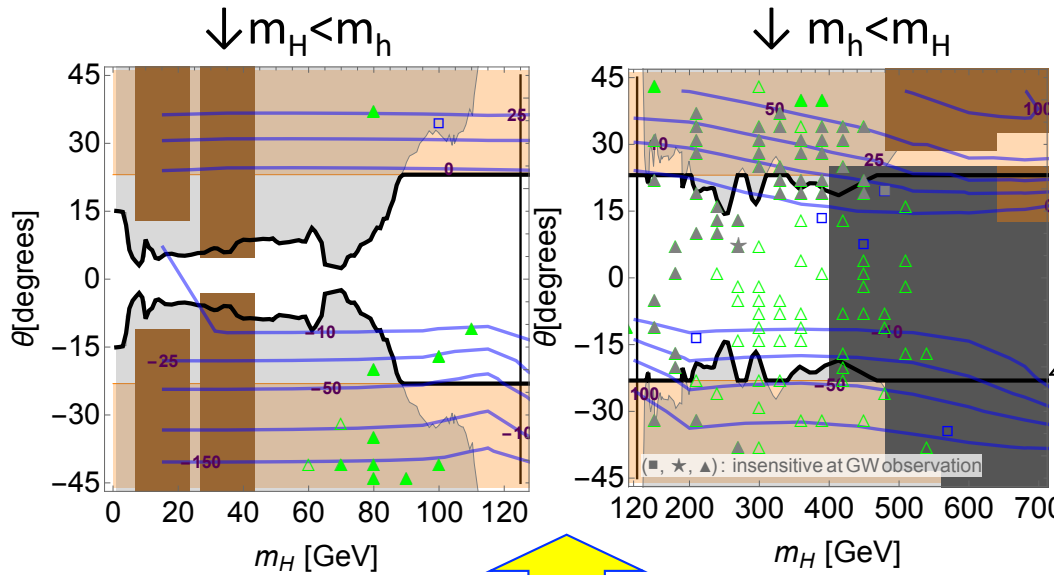
Sensitivities

- DECIGO [S.Kawamura, et al., Class. Quant. Grav. **28**, 094011 (2011)]
- eLISA [C.Caprini et al., arXiv:1512.06239 (JCAP)]

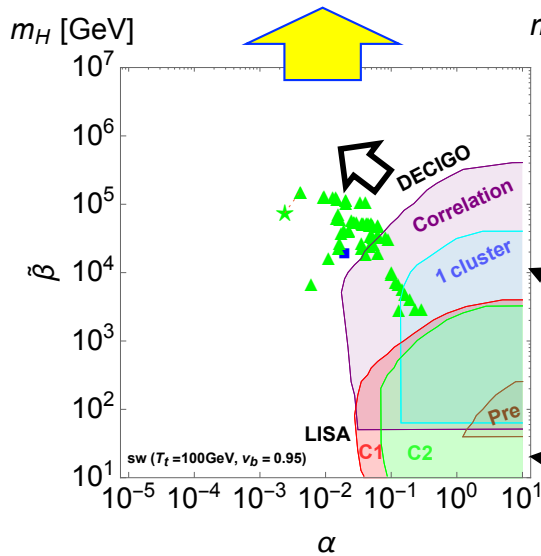
A numerical result on (m_H, θ) by fixing (m_X, g_X)

Hashino, Kakizaki, Kanemura, Ko, TM, 1802.02947

$m_X=200\text{GeV}, g_X=2$ ($v_S=100\text{GeV}$) as an example



Categories	Symbols	Legends
Theory	[Brown shaded]	excluded by perturbative unitarity
		excluded by vacuum stability
	[Blue line]	contours of $\Delta\lambda_{hhh}/\lambda_{hhh}^{\text{SM}}$ (%)
		combined exclusion limit ([Orange shaded] + [Grey shaded])
Collider	[Orange shaded]	constraint by the κ_Z measurement (see Eq. (4.3))
	[Grey shaded]	constraint by the direct searches for the H -boson (see Ref. [119])
	[Black line]	
	[Blue shaded]	
	[Grey shaded]	
PT	[Blue square]	one-step PT (1st order)
	[Blue square]	one-step PT (2nd order)
	[Green star]	two-step PT (1st order \rightarrow 1st order)
	[Green triangle]	two-step PT (2nd order \rightarrow 1st order)
	[Green triangle]	two-step PT (1st order \rightarrow 2nd order)
GW	[Pink shaded]	DECIGO (Correlation)
	[Light blue shaded]	DECIGO (1 cluster)
	[Light brown shaded]	DECIGO (Pre)
	[Red shaded]	LISA (C1)
	[Green shaded]	LISA (C2)

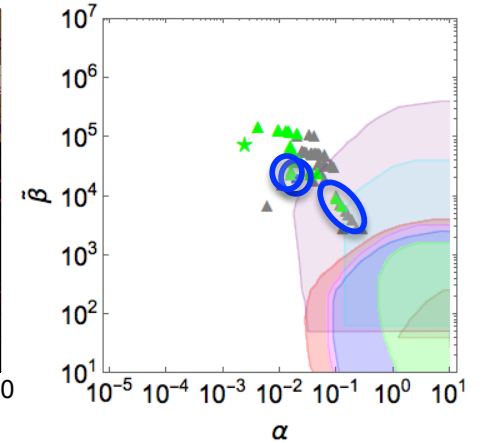
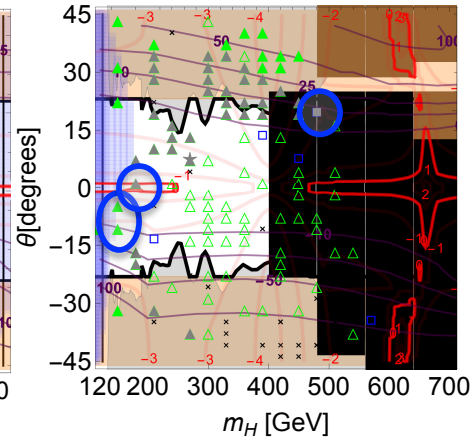
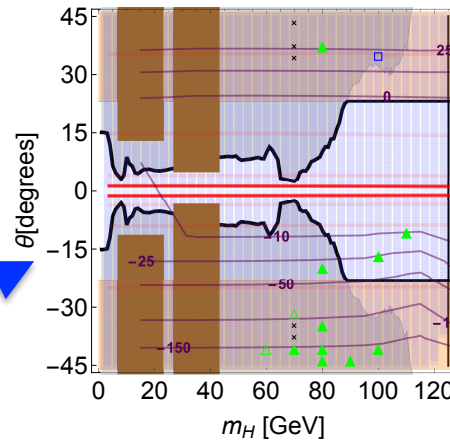
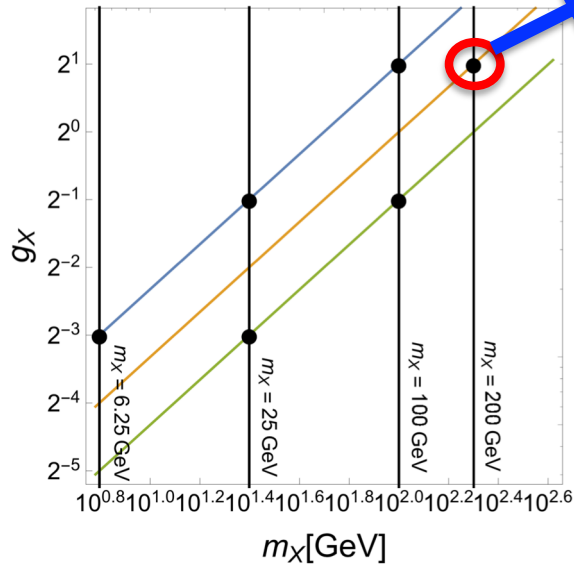


Sensitivities

- DECIGO [S.Kawamura, et al., Class. Quant. Grav. **28**, 094011 (2011)]
- eLISA [C.Caprini et al., arXiv:1512.06239 (JCAP)]

On other benchmark points

$(m_X [\text{GeV}], g_X)_{\text{vs}}$	#	PT	GW	DM
$(200, 2^1)_{100\text{GeV}}$	1	C	○	△
	2	C	△	○
	3	D	△	△
$(100, 2^1)_{50\text{GeV}}$	4	C	○	excluded by XENON1T
$(100, 2^{-1})_{200\text{GeV}}$	5	C	○	excluded by XENON1T
	6	D	excluded by collider	excluded by XENON1T
$(25, 2^{-1})_{50\text{GeV}}$	7	C	○	excluded by XENON1T
$(25, 2^{-3})_{200\text{GeV}}$	8	C	excluded by collider	excluded by XENON1T
$(6.25, 2^{-3})_{50\text{GeV}}$	9	D	excluded by collider	excluded by XENON1T



On other benchmark points

$(m_X [\text{GeV}], g_X)_{v_s}$	#	PT	GW	DM
$(200, 2^1)_{100\text{GeV}}$	1	C	○	△
	2	C	△	○
	3	D	△	△
$(100, 2^1)_{50\text{GeV}}$	4	C	○	excluded by XENON1T
	5	C	○	excluded by XENON1T
$(100, 2^{-1})_{200\text{GeV}}$	6	D	excluded by collider	excluded by XENON1T
$(25, 2^{-1})_{50\text{GeV}}$	7	C	○	excluded by XENON1T
$(25, 2^{-3})_{200\text{GeV}}$	8	C	excluded by collider	excluded by XENON1T
$(6.25, 2^{-3})_{50\text{GeV}}$	9	D	excluded by collider	excluded by XENON1T

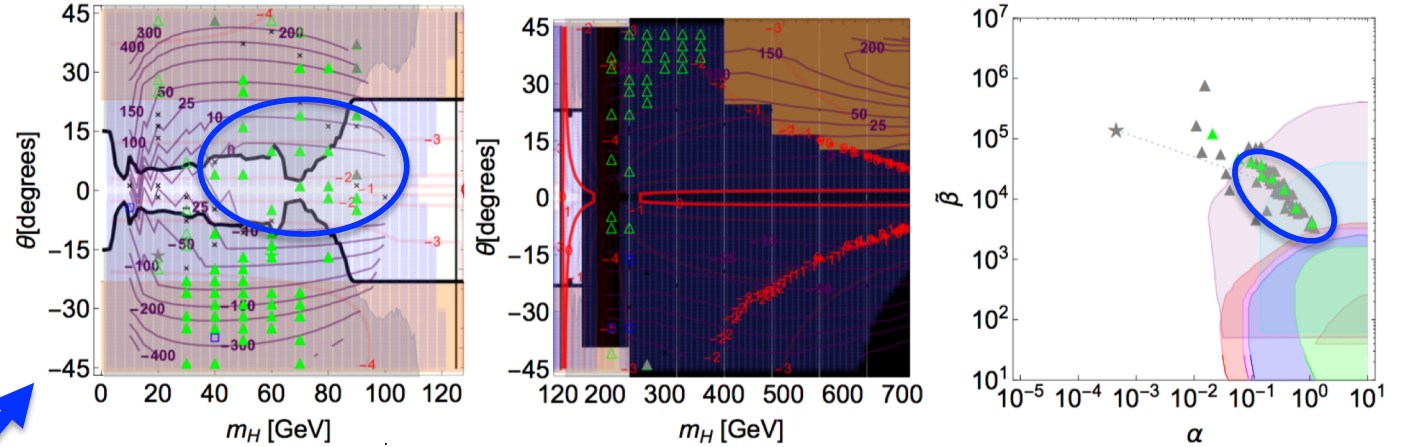


FIG. 5: $m_X = 100 \text{ GeV}$, $g_X = 2^1$ ($v_S = 50 \text{ GeV}$). See the caption in Figs. 3–4.

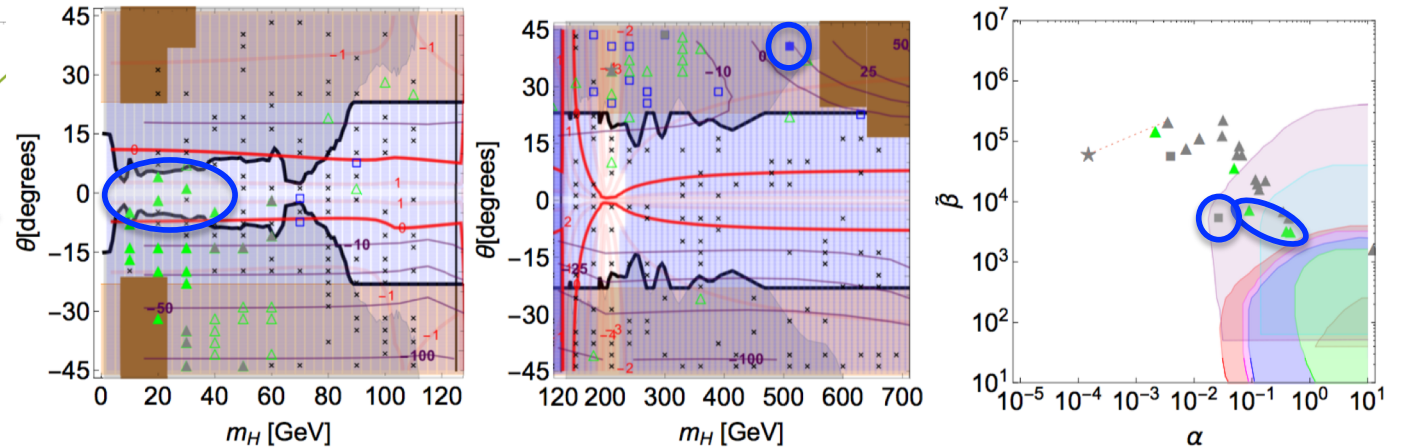
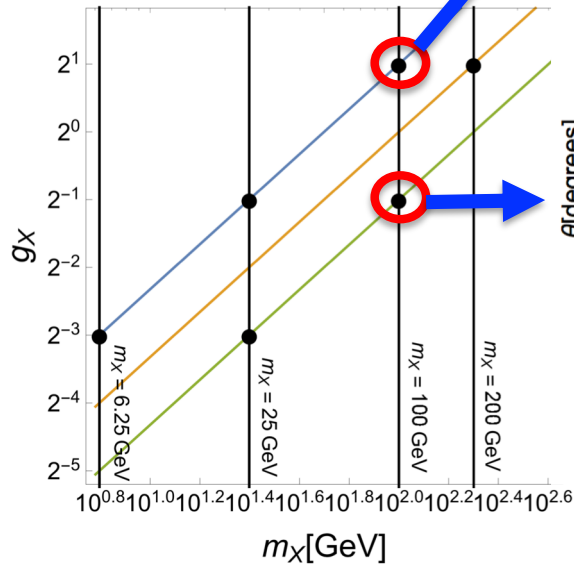


FIG. 6: $m_X = 100 \text{ GeV}$, $g_X = 2^{-1}$ ($v_S = 200 \text{ GeV}$). See the caption in Figs. 3–4.

On other benchmark points

$(m_X [\text{GeV}], g_X)_{v_S}$	#	PT	GW	DM
$(200, 2^1)_{100\text{GeV}}$	1	C	○	△
	2	C	△	○
	3	D	△	△
$(100, 2^1)_{50\text{GeV}}$	4	C	○	excluded by XENON1T
$(100, 2^{-1})_{200\text{GeV}}$	5	C	○	excluded by XENON1T
$(25, 2^{-1})_{50\text{GeV}}$	6	D	excluded by collider	excluded by XENON1T
	7	C	○	excluded by XENON1T
$(25, 2^{-3})_{200\text{GeV}}$	8	C	excluded by collider	excluded by XENON1T
$(6.25, 2^{-3})_{50\text{GeV}}$	9	D	excluded by collider	excluded by XENON1T

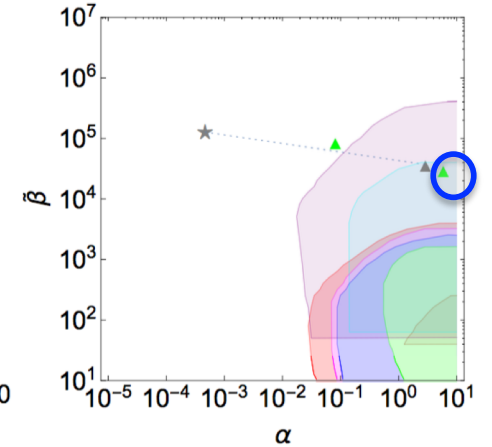
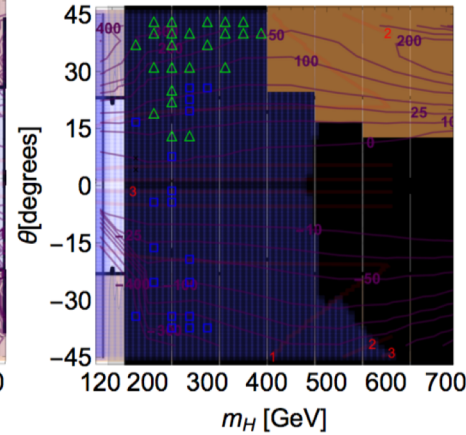
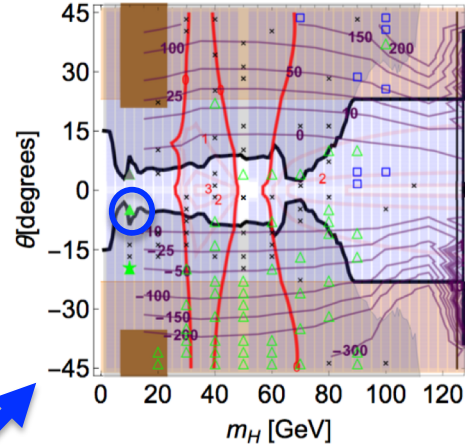


FIG. 7: $m_X = 25 \text{ GeV}$, $g_X = 2^{-1}$ ($v_S = 50 \text{ GeV}$). See the caption in Figs. 3–4.

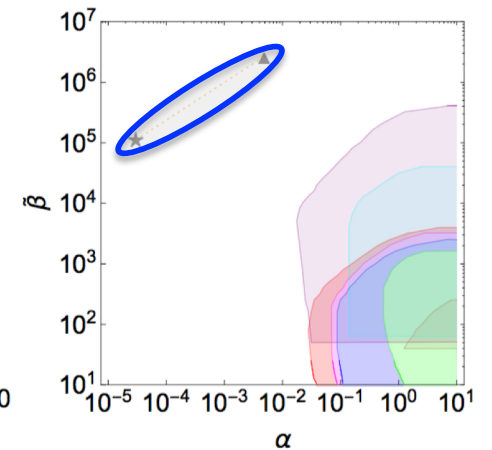
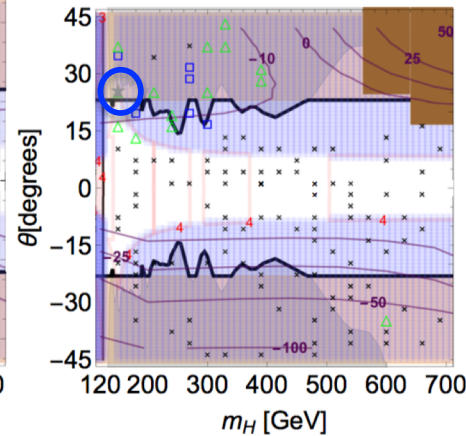
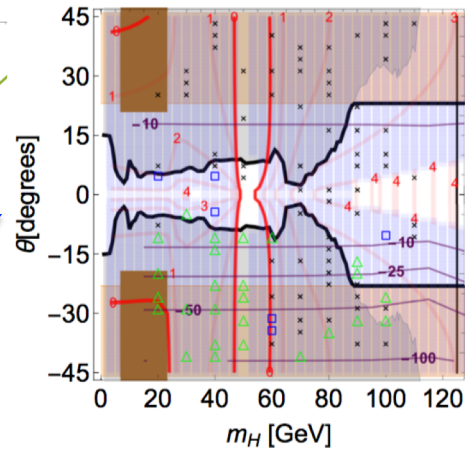
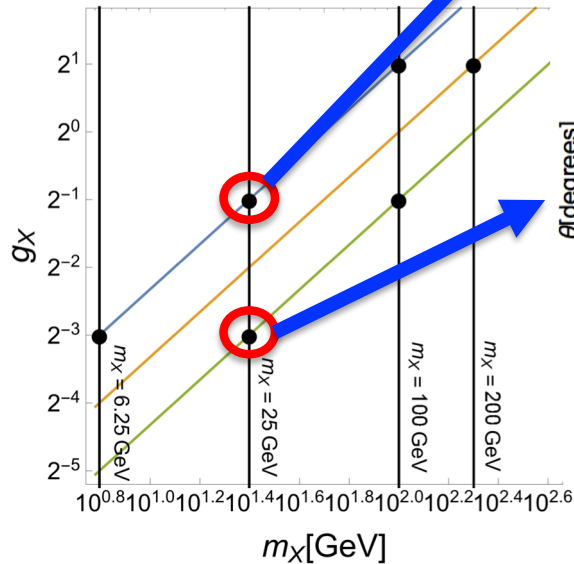


FIG. 8: $m_X = 25 \text{ GeV}$, $g_X = 2^{-3}$ ($v_S = 200 \text{ GeV}$). See the caption in Figs. 3–4.

On other benchmark points

$(m_X [\text{GeV}], g_X)_{v_S}$	#	PT	GW	DM
$(200, 2^1)_{100\text{GeV}}$	1	C	○	△
	2	C	△	○
	3	D	△	△
$(100, 2^1)_{50\text{GeV}}$	4	C	○	excluded by XENON1T
$(100, 2^{-1})_{200\text{GeV}}$	5	C	○	excluded by XENON1T
	6	D	○	excluded by XENON1T
$(25, 2^{-1})_{50\text{GeV}}$	7	C	○	excluded by XENON1T
$(25, 2^{-3})_{200\text{GeV}}$	8	C	○	excluded by XENON1T
$(6.25, 2^{-3})_{50\text{GeV}}$	9	D	○	excluded by XENON1T

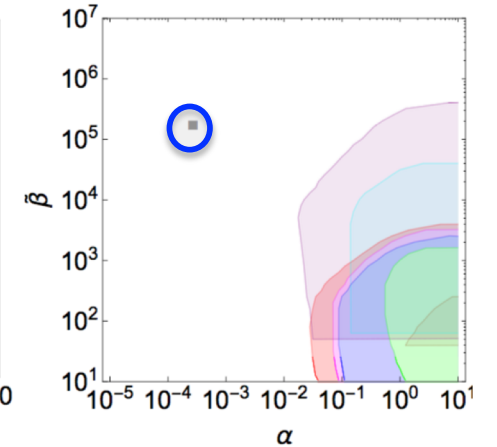
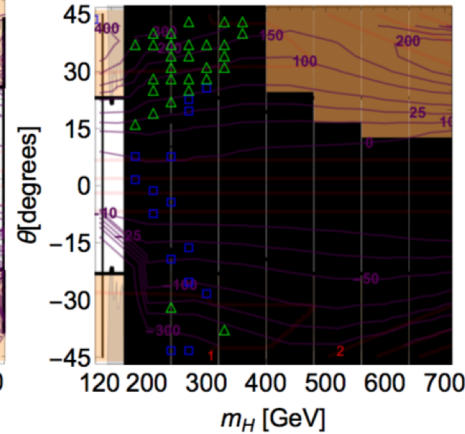
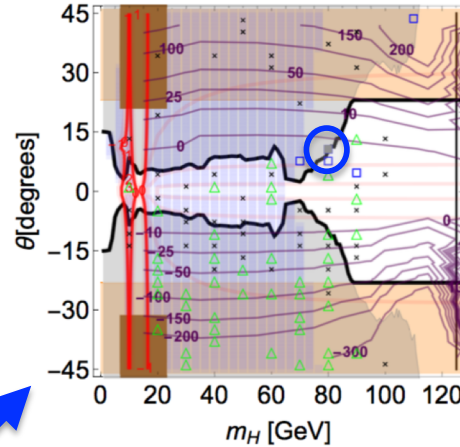
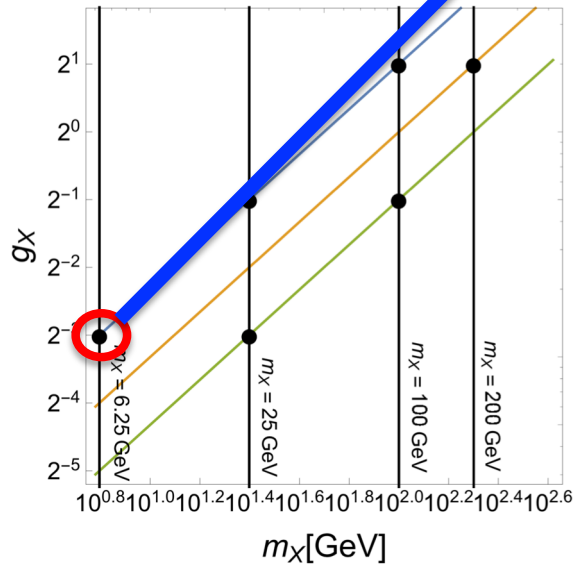


FIG. 9: $m_X = 6.25 \text{ GeV}$, $g_X = 2^{-3}$ ($v_S = 50 \text{ GeV}$). See the caption in Figs. 3–4.



Higgs portal DM

Higgs portal DM (effective field theory)

Kanemura, Matsumoto, Nabeshima, Okada (1005.5651),
Djouadi, Lebedev, Mambrini, Quevillon (1112.3299), ...

Singlet scalar DM

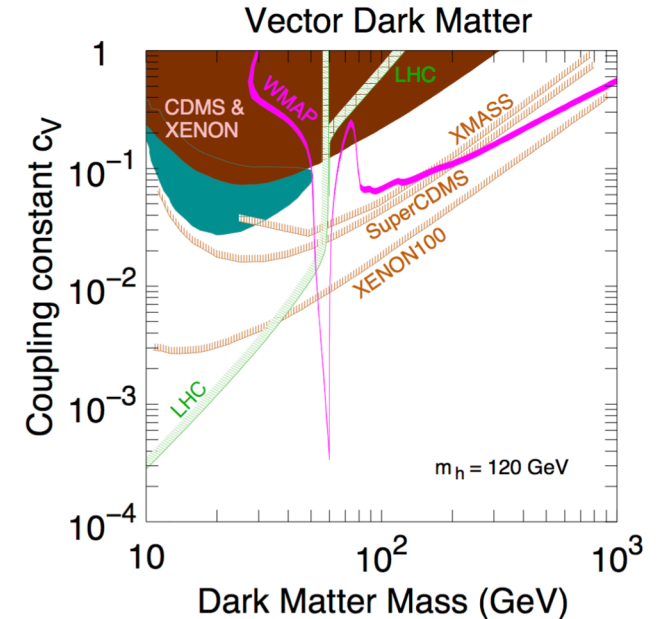
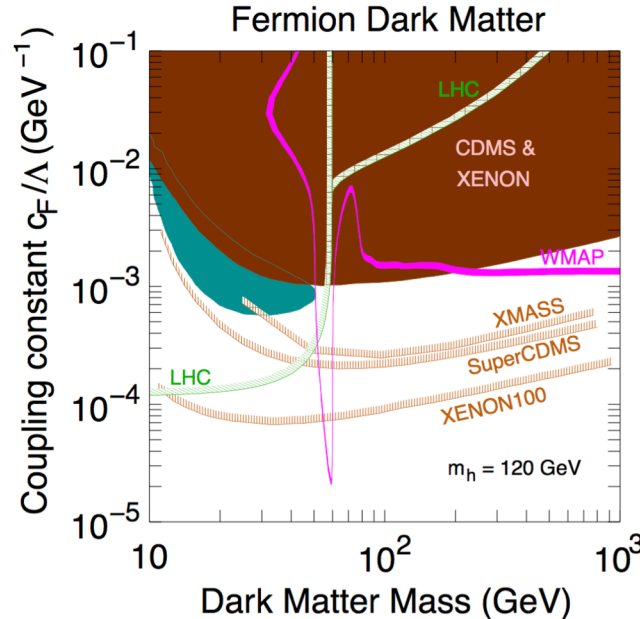
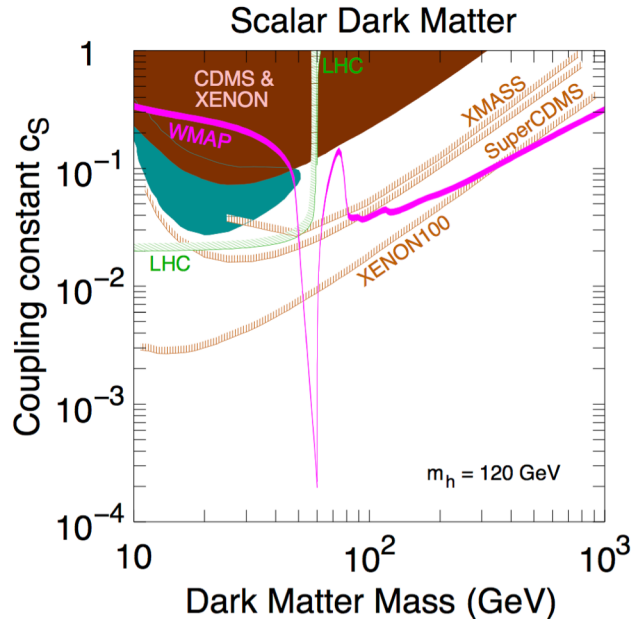
$$\mathcal{L}_{\text{SSDM}}^{\text{EFT}} = \frac{1}{2}(\partial_\mu S)^2 - \frac{1}{2}m_S^2 S^2 - \frac{1}{4}\lambda_S S^4 - \frac{c_S}{2}S^2|H|^2$$

Singlet Fermion DM

$$\mathcal{L}_{\text{SFDM}}^{\text{EFT}} = \bar{\chi}(i\not{\partial} - m_\chi)\chi - \frac{c_F}{2\Lambda}\bar{\chi}\chi|H|^2$$

Vector DM

$$\mathcal{L}_{\text{VDM}}^{\text{EFT}} = -\frac{1}{4}V_{\mu\nu}V^{\mu\nu} + \frac{1}{2}m_V^2 V_\mu V^\mu - \frac{1}{4}\lambda_V(V_\mu V^\mu)^2 - \frac{c_V}{2}V_\mu V^\mu|H|^2$$



$$\Phi = \begin{pmatrix} w^+ \\ \frac{1}{\sqrt{2}}(v_\Phi + \phi_1 + iz) \end{pmatrix}$$

Higgs portal DM (renormalizable model) with 1stOPT

Singlet scalar DM (5 parameters) $\mathcal{L}_{\text{SSDM}} = -V_0(\Phi, S)$ [1210.4196](#), [1409.0005](#), [1611.02073](#), [1702.06124](#), [1704.03381](#), ...

$$V_0(\Phi, S) = -\mu_\Phi^2 |\Phi|^2 + \frac{1}{2} \mu_S^2 S^2 + \lambda_\Phi |\Phi|^4 + \frac{1}{4} \lambda_S S^4 + \frac{1}{2} \lambda_{\Phi S} |\Phi|^2 S^2 \quad \langle S \rangle = 0$$

Scalar potential is imposed unbroken Z_2 symmetry.

$$m_S^2 = \mu_S^2 + \lambda_{HS} v^2$$

PT can be caused by thermal loop effect, but excluded by DM direct searches.

Singlet Fermion DM (10 parameters)

$$\mathcal{L}_{\text{SFDM}} = \bar{\psi}(i\partial - \underline{m_{\psi_0}})\psi - \underline{\lambda S} \bar{\psi}\psi - V_0(\Phi, S) \quad \begin{matrix} 1112.1847, 1209.4163, \\ 1305.3452, 1402.3087, \dots \end{matrix}$$

$$V_0(\Phi, S) = -\mu_\Phi^2 |\Phi|^2 + \lambda_\Phi |\Phi|^4 + \mu_{\Phi S} |\Phi|^2 S + \frac{\lambda_{\Phi S}}{2} |\Phi|^2 S^2 + \mu_S^3 S + \frac{m_S^2}{2} S^2 + \frac{\mu'_S}{3} S^3 + \frac{\lambda_S}{4} S^4 \quad \begin{matrix} S = v_S + \phi_2 \\ m_\psi \equiv m_{\psi_0} + \lambda v_S \end{matrix}$$

Vector DM (6 parameters)

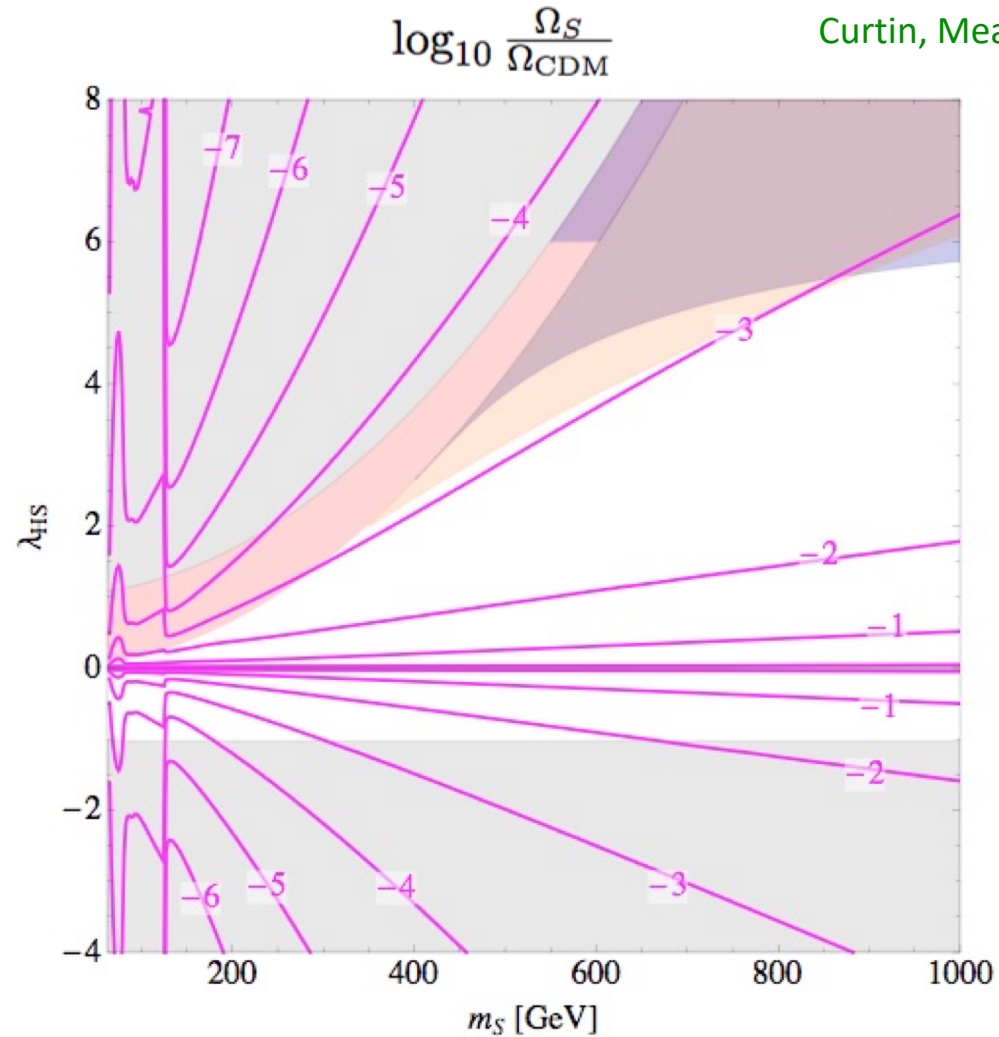
$$\mathcal{L}_{\text{VDM}} = -\frac{1}{4} X_{\mu\nu} X^{\mu\nu} + |D_\mu S|^2 - V_0(\Phi, S) \quad 1212.2131, 1412.3823, \dots$$

$$V_0(\Phi, S) = -\mu_\Phi^2 |\Phi|^2 - \mu_S^2 |S|^2 + \lambda_\Phi |\Phi|^4 + \lambda_S |S|^4 + \lambda_{\Phi S} |\Phi|^2 |S|^2 \quad S = \frac{1}{\sqrt{2}}(v_S + \phi_2 + ix)$$

$$D_\mu S = (\partial_\mu + i \underline{g_X} Q_S X_\mu) S \longrightarrow m_X = g_X |Q_S| v_S$$

1stOPT in scalar DM model is excluded by XENON1T

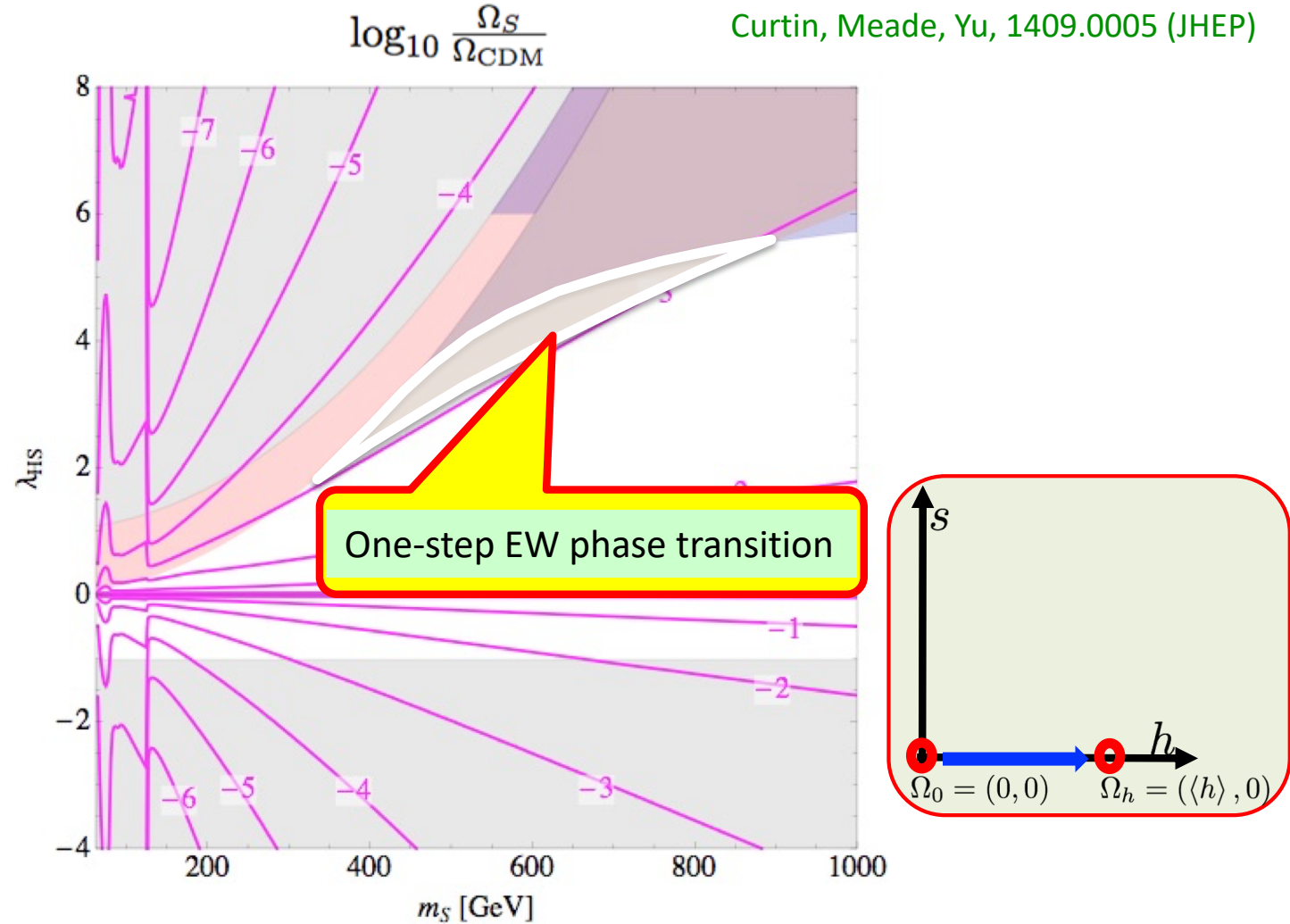
Curtin, Meade, Yu, 1409.0005 (JHEP)



See also Beniwal, Lewicki, Wells, White, Williams, 1702.06124 (JHEP)

1stOPT in scalar DM model is excluded by XENON1T

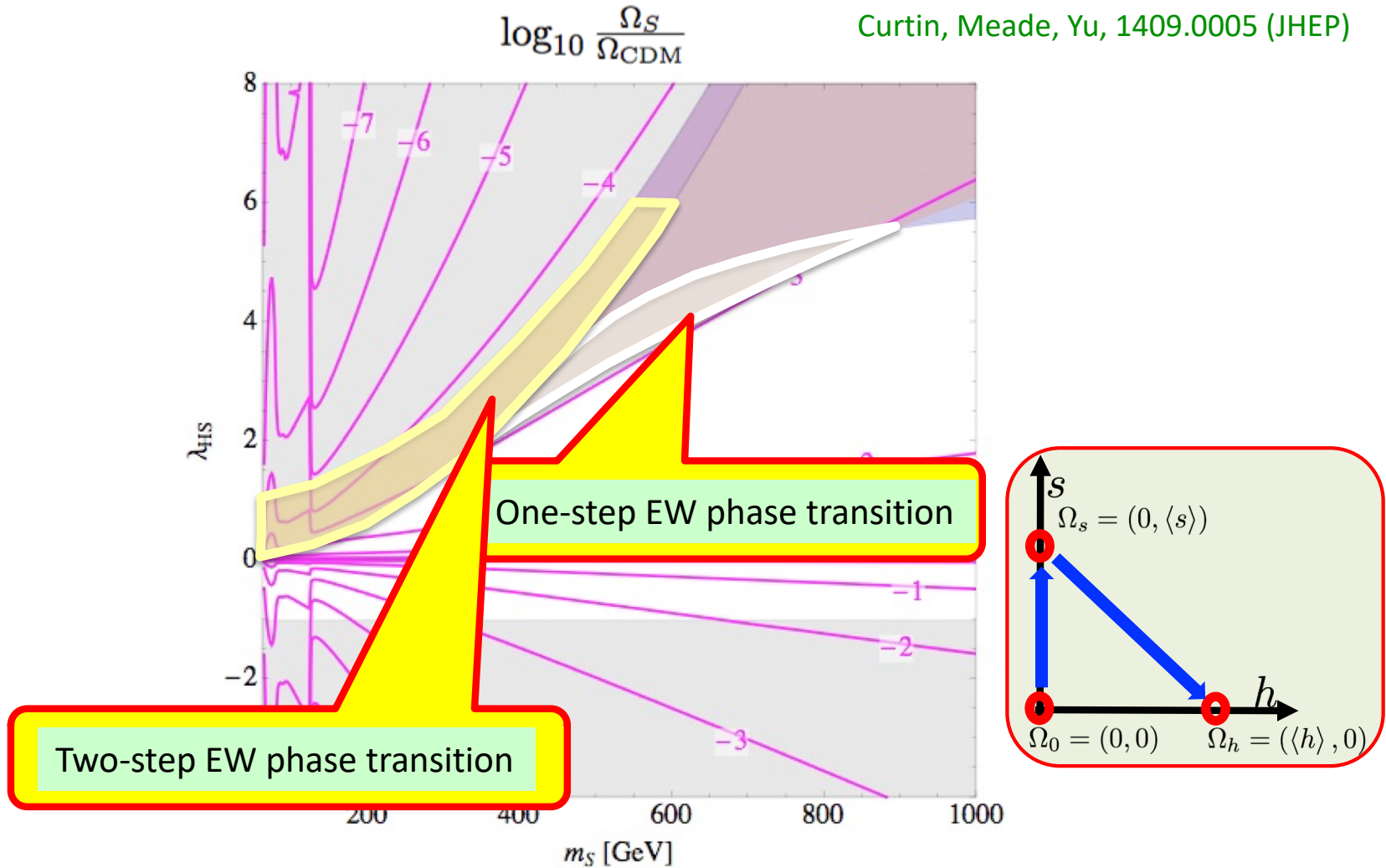
Curtin, Meade, Yu, 1409.0005 (JHEP)



See also Beniwal, Lewicki, Wells, White, Williams, 1702.06124 (JHEP)

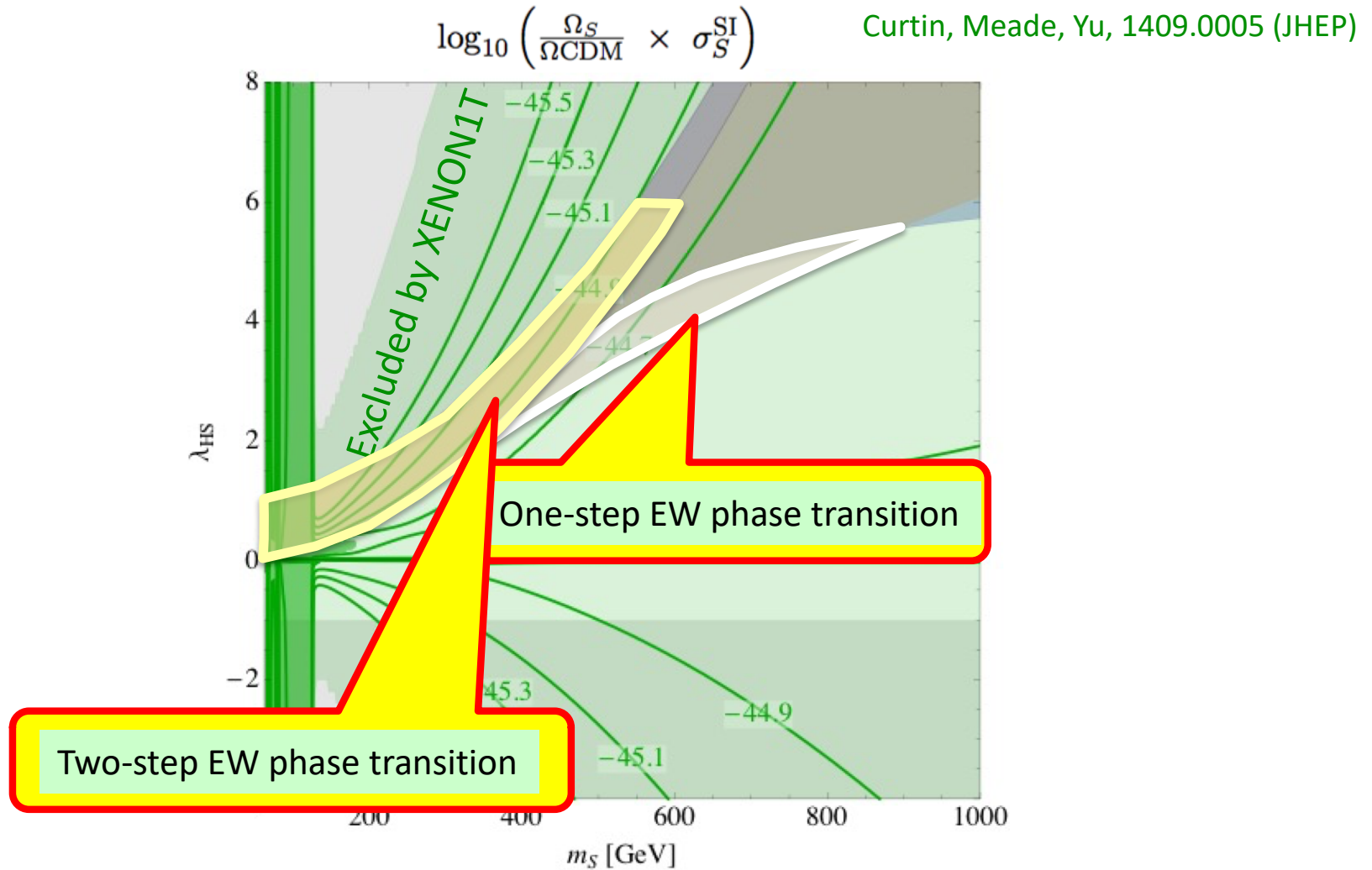
1stOPT in scalar DM model is excluded by XENON1T

Curtin, Meade, Yu, 1409.0005 (JHEP)



See also Beniwal, Lewicki, Wells, White, Williams, 1702.06124 (JHEP)

1stOPT in scalar DM model is excluded by XENON1T



See also Beniwal, Lewicki, Wells, White, Williams, 1702.06124 (JHEP)

$$\Phi = \begin{pmatrix} w^+ \\ \frac{1}{\sqrt{2}}(v_\Phi + \phi_1 + iz) \end{pmatrix}$$

Higgs portal DM (renormalizable model) with 1stOPT

Singlet scalar DM (5 parameters) $\mathcal{L}_{\text{SSDM}} = -V_0(\Phi, S)$ [1210.4196](#), [1409.0005](#), [1611.02073](#),
[1702.06124](#), [1704.03381](#), ...

$$V_0(\Phi, S) = -\mu_\Phi^2 |\Phi|^2 + \frac{1}{2} \mu_S^2 S^2 + \lambda_\Phi |\Phi|^4 + \frac{1}{4} \lambda_S S^4 + \frac{1}{2} \lambda_{\Phi S} |\Phi|^2 S^2 \quad \langle S \rangle = 0$$

$$m_S^2 = \mu_S^2 + \lambda_{HS} v^2$$

Scalar potential is imposed unbroken Z_2 symmetry.

PT can be caused by thermal loop effect, but excluded by DM direct searches.

Singlet Fermion DM (10 parameters)

$$\mathcal{L}_{\text{SFDM}} = \bar{\psi}(i\not{\partial} - \underline{m_{\psi_0}})\psi - \underline{\lambda S} \bar{\psi}\psi - V_0(\Phi, S) \quad \text{1112.1847, 1209.4163, 1305.3452, 1402.3087, ...}$$

$$V_0(\Phi, S) = -\mu_\Phi^2 |\Phi|^2 + \lambda_\Phi |\Phi|^4 + \mu_{\Phi S} |\Phi|^2 S + \frac{\lambda_{\Phi S}}{2} |\Phi|^2 S^2 + \mu_S^3 S + \frac{m_S^2}{2} S^2 + \frac{\mu'_S}{3} S^3 + \frac{\lambda_S}{4} S^4 \quad \begin{matrix} S = v_S + \phi_2 \\ m_\psi \equiv m_{\psi_0} + \lambda v_S \end{matrix}$$

Scalar potential is general shape with a real Higgs singlet scalar field (Higgs singlet model; HSM).

PT can be caused by tree level (mixing) effect of the scalar potential. DM contributes as the loop effect.

Vector DM (6 parameters)

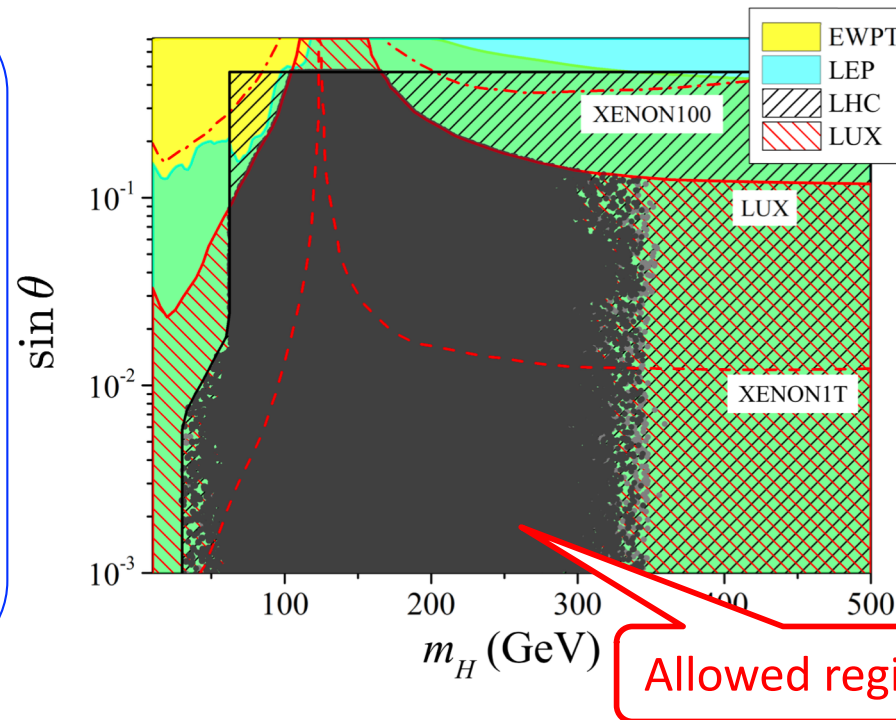
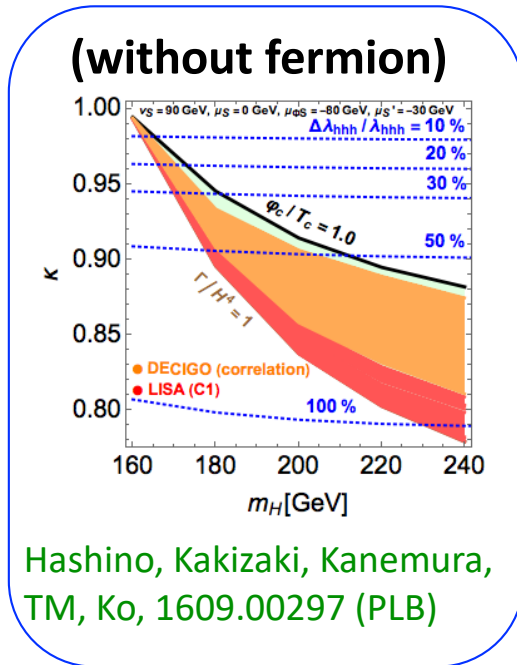
$$\mathcal{L}_{\text{VDM}} = -\frac{1}{4} X_{\mu\nu} X^{\mu\nu} + |D_\mu S|^2 - V_0(\Phi, S) \quad \text{1212.2131, 1412.3823, ...}$$

$$V_0(\Phi, S) = -\mu_\Phi^2 |\Phi|^2 - \mu_S^2 |S|^2 + \lambda_\Phi |\Phi|^4 + \lambda_S |S|^4 + \lambda_{\Phi S} |\Phi|^2 |S|^2 \quad S = \frac{1}{\sqrt{2}}(v_S + \phi_2 + ix)$$

$$D_\mu S = (\partial_\mu + i \underline{g_X} Q_S X_\mu) S \longrightarrow m_X = g_X |Q_S| v_S$$

1stOPT in Fermion DM model

Li, Zhou, 1402.3087 (JHEP)



$$m_H \simeq 30 - 250 \text{ GeV}$$

$$\theta \lesssim 28^\circ (\sin \theta = 0.47)$$

$$m_\psi = 15 - 350 \text{ GeV}$$

Figure 8. Allowed region in the $m_H - \sin \theta$ plane satisfying $\varphi_c/T_c > 1$ and all the constraints from the electroweak precision test (EWPT) at 95% CL, the LEP data at 95% CL, the Higgs search results at LHC, and the upper bound on DM-nucleon scattering cross section from the LUX experiment. The red dot-dashed line is the upper bound on the mixing angle from the 90% CL XENON100 constraint and the red dashed line is that from the projected exclusion limit of the future XENON1T experiment. The dots are the sample points satisfying $\varphi_c/T_c > \mathcal{E}$ and all the constraints with $\mathcal{E} = 1.2$ (dark gray) and $\mathcal{E} = 1$ (light gray), respectively.

Gravitational wave observations

Gravitational waves from 1stOPT

Sketch of first order phase transition

Effective potential at one-loop level:

$$V_{\text{eff}}(\varphi) = -\frac{\mu^2}{2}\varphi^2 + \frac{\lambda}{4}\varphi^4 + \sum_i \frac{n_i}{64\pi^2} M_i^4(\varphi) \left(\ln \frac{M_i^2(\varphi)}{Q^2} - \frac{3}{2} \right)$$

Contribution at finite-temperatures:

$$\Delta V_T(\varphi, T) = \frac{T^4}{2\pi^2} \left[\sum_{i=\text{bosons}} n_i I_B(a^2) + \sum_{i=\text{fermions}} n_i I_F(a^2) \right]$$

$$I_{B/F}(a^2) = \int_0^\infty dx x^2 \ln \left(1 \mp e^{-\sqrt{x^2+a^2}} \right) \quad a^2 = \frac{M^2(\varphi, T)}{T^2}$$

High-temperature expansion:

$$V_{\text{eff}}(\varphi, T) \simeq D(T^2 - T_0^2)\varphi^2 - \underline{ET}\varphi^3 + \frac{\lambda_T}{4}\varphi^4 + \dots \quad \varphi_c/T_c \propto E$$

$$I_B(a^2) = -\frac{\pi^4}{45} + \frac{\pi^2}{12}a^2 - \frac{\pi}{6}(a^2)^{3/2} - \frac{a^4}{32} \left(\ln \frac{a^2}{\alpha_B} - 3/2 \right) + \mathcal{O}(a^6)$$

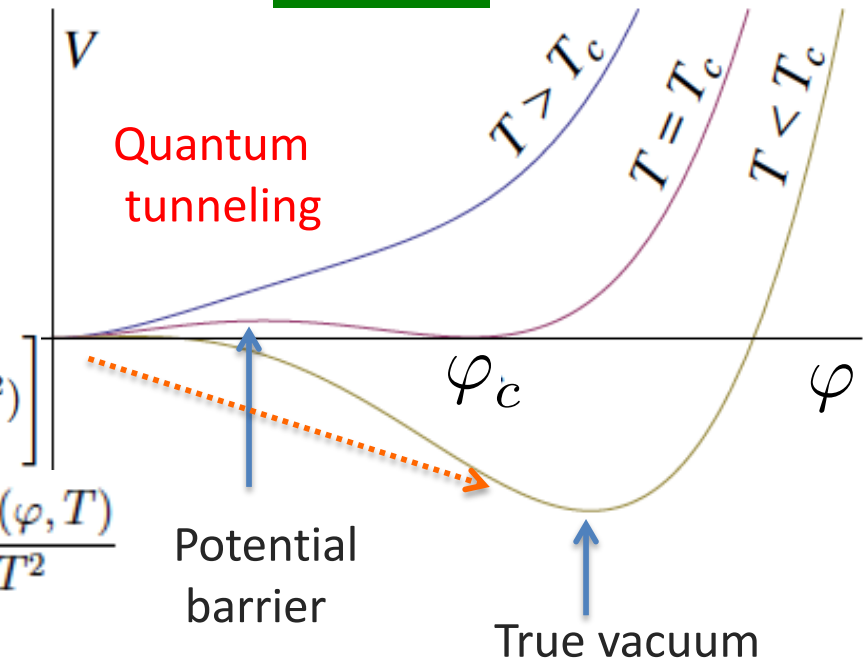
$$I_F(a^2) = \frac{7\pi^4}{360} - \frac{\pi^2}{24}a^2 - \frac{a^4}{32} \left(\ln \frac{a^2}{\alpha_F} - 3/2 \right) + \mathcal{O}(a^6)$$

Bosonic loop contribute to the cubic term

Strongly 1st OPT ($\varphi_c/T_c \gtrsim 1$) can be achieved by adding bosons

Necessary for successful electroweak baryogenesis

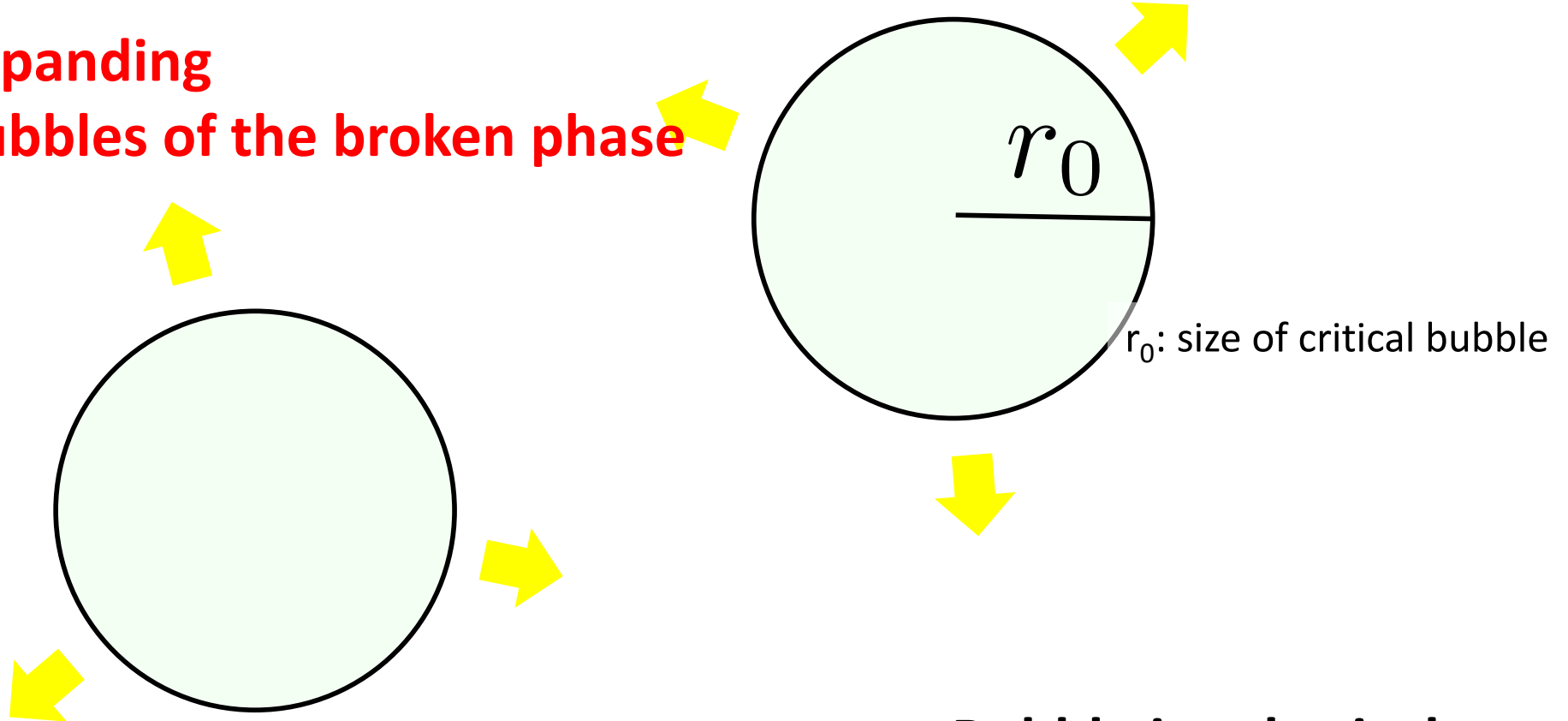
1st OPT



GWs from 1stOPT

C. Caprini *et al.*, 1512.06239 (JCAP)

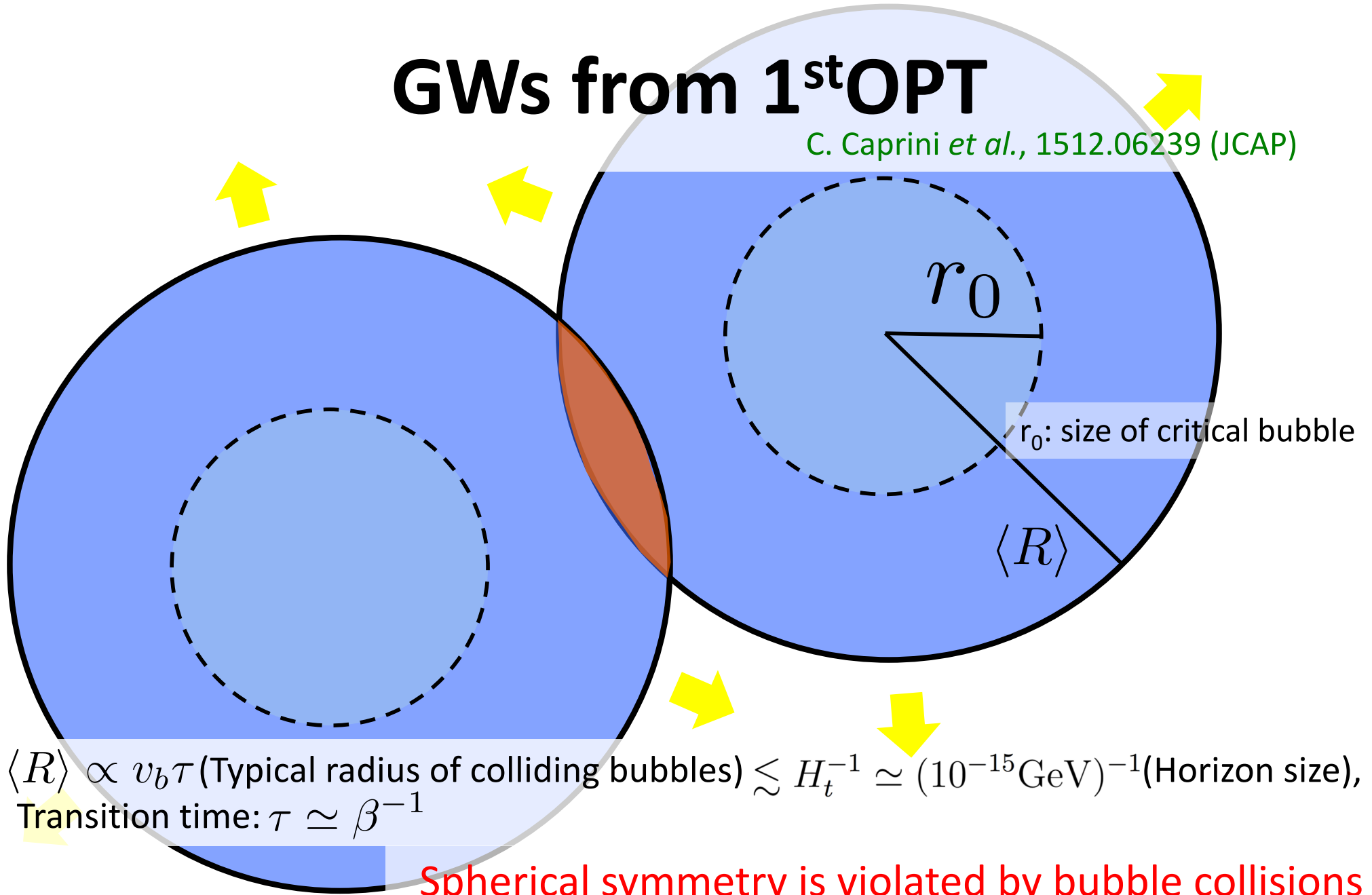
Expanding
bubbles of the broken phase



Bubble is spherical
No GW occurs

GWs from 1stOPT

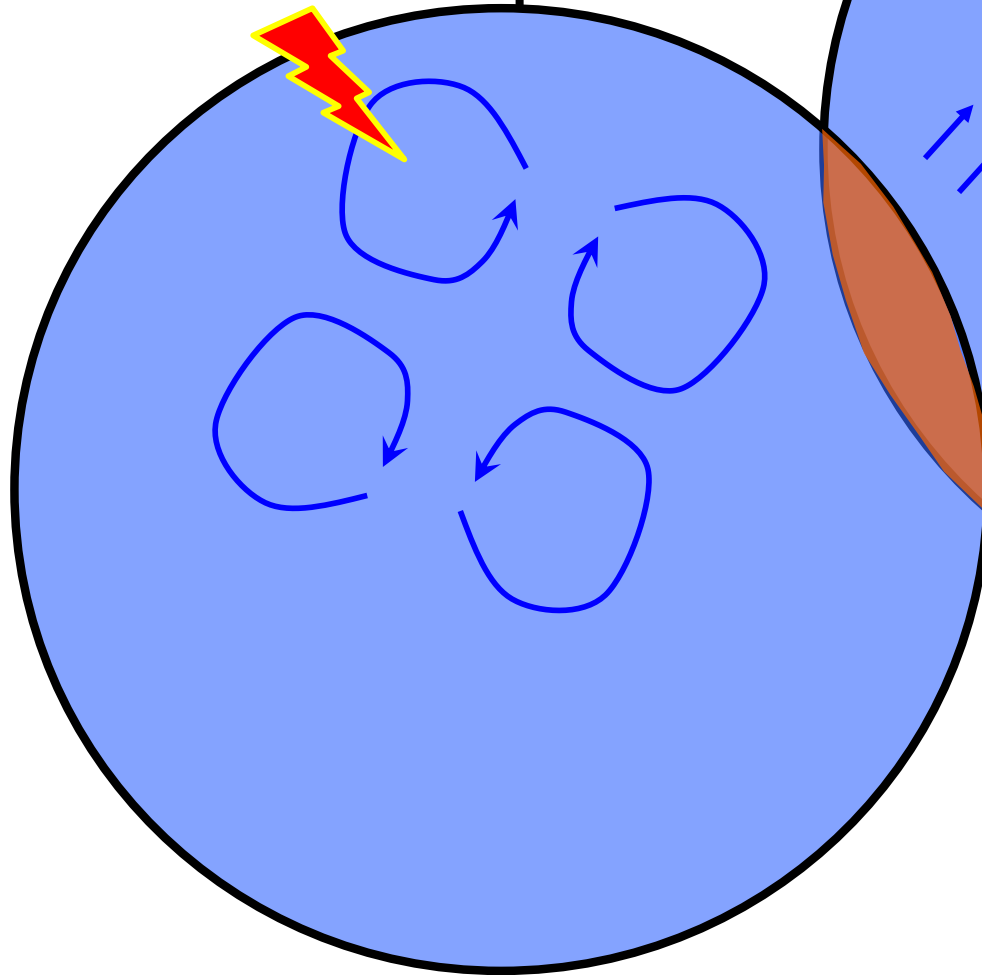
C. Caprini *et al.*, 1512.06239 (JCAP)



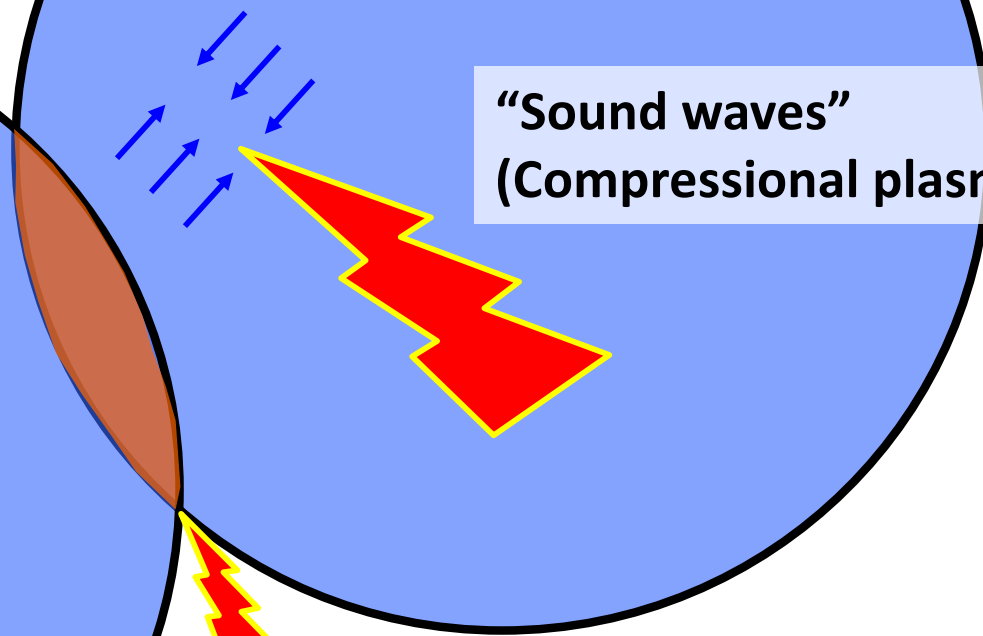
GWs from 1stOPT

C. Caprini *et al.*, 1512.06239 (JCAP)

“Magnetohydrodynamic
turbulence in the plasma”



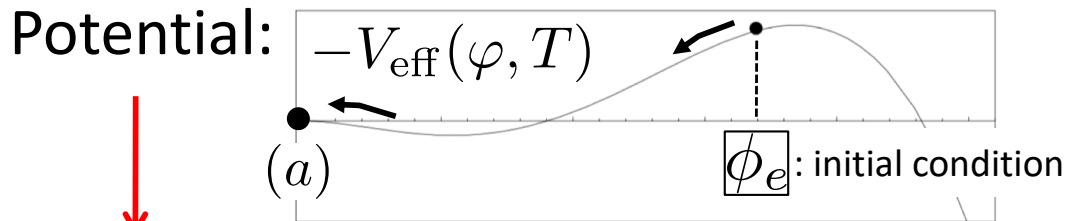
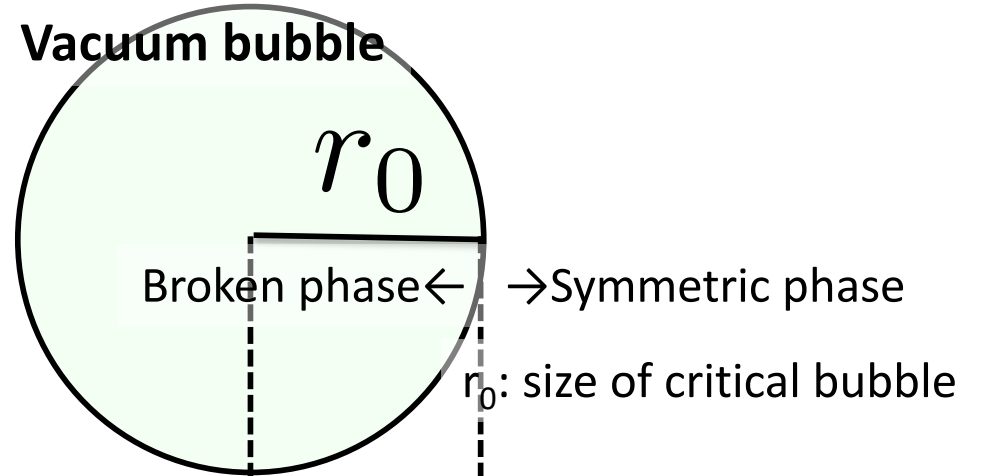
“Sound waves”
(Compressional plasma)



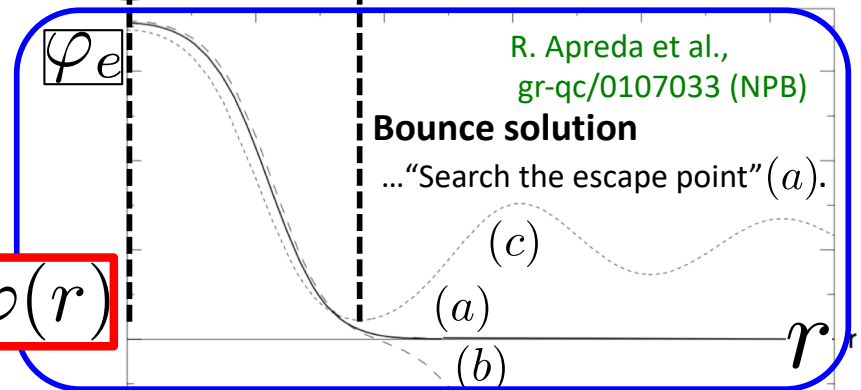
“Bubble collision”
(Envelope approximation)



Bubble configuration



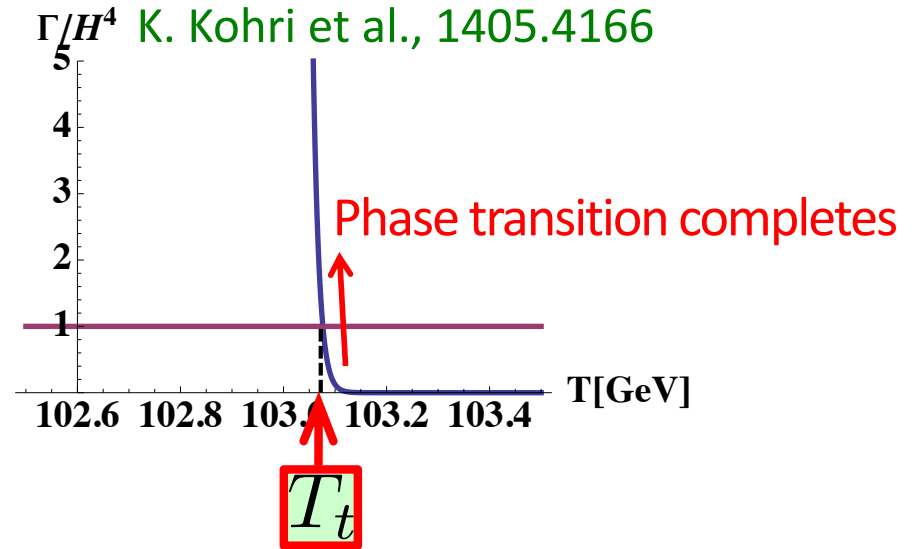
Eq. of motion: $\frac{d^2\varphi}{dr^2} + \frac{2}{r} \frac{d\varphi}{dr} - \frac{dV_{\text{eff}}}{d\varphi} = 0 \rightarrow \varphi(r)$



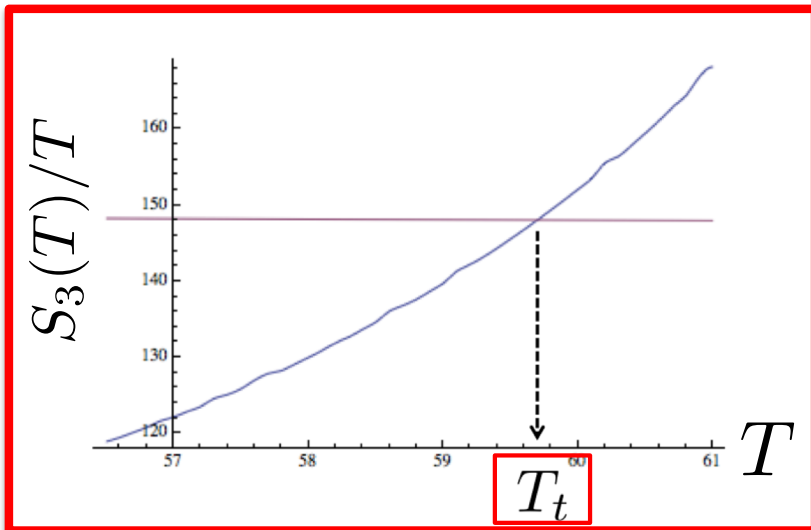
$\varphi(r)$ each $T \rightarrow$ Bubble nucleation rate: $\Gamma(T) \simeq T^4 e^{-\frac{S_3(T)}{T}}$

3-dim. Euclidean action: $S_3(T) = \int dr^3 \left\{ \frac{1}{2} (\vec{\nabla}\varphi)^2 + V_{\text{eff}}(\varphi, T) \right\}$

Transition temperature



Definition of phase transition temperature T_t



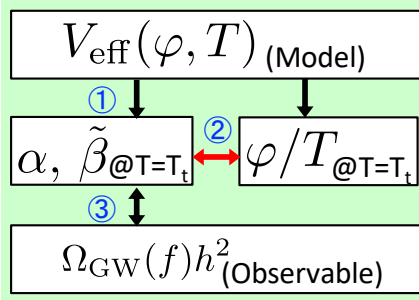
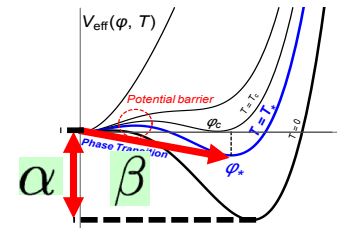
$$\left. \frac{\Gamma}{H^4} \right|_{T=T_t} \simeq 1 \iff \left. \frac{S_3(T)}{T} \right|_{T=T_t} \simeq 140 - 150$$

(H : Hubble parameter)

$$\Gamma(T) \simeq T^4 e^{-\frac{S_3(T)}{T}}$$

$$S_3(T) = \int dr^3 \left\{ \frac{1}{2} (\vec{\nabla} \varphi)^2 + V_{\text{eff}}(\varphi, T) \right\}$$

GWs from 1stOPT



~ Probing the Higgs potential by GW observations ~

Characteristic parameters of 1stOPT

• α is defined as $\alpha \equiv \frac{\epsilon}{\rho_{\text{rad}}}\bigg|_{T=T_t}$. (ρ_{rad} is energy density of rad.)

- Latent heat: $\epsilon(T) \equiv -\Delta V_{\text{eff}}(\varphi_B(T), T) + T \frac{\partial \Delta V_{\text{eff}}(\varphi_B(T))}{\partial T}$

$\alpha \sim$ “Normalized difference of the potential minima”

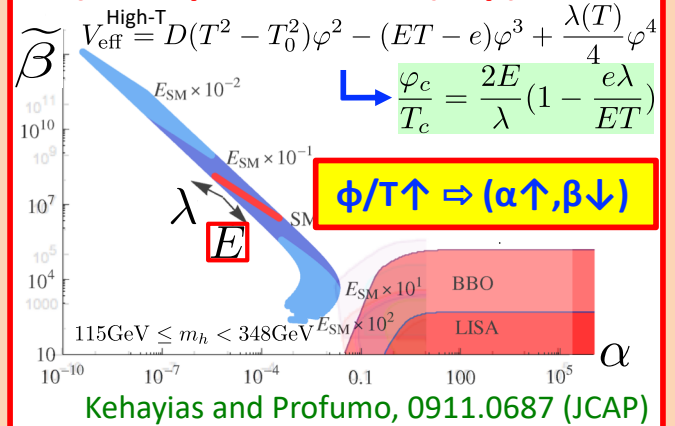
• β is defined as $\beta \equiv \frac{1}{\Gamma} \frac{d\Gamma}{dt}\bigg|_{t=t_t} \rightarrow \tilde{\beta} \left(\equiv \frac{\beta}{H_t} \right) = T_t \frac{d(S_3(T)/T)}{dT}\bigg|_{T=T_t}$

- Bubble nucleation rate: $\Gamma(T) \simeq T^4 e^{-\frac{S_3(T)}{T}}$

- 3-dim. Euclidean action: $S_3(T) = \int dr^3 \left\{ \frac{1}{2} (\vec{\nabla}\varphi)^2 + V_{\text{eff}}(\varphi, T) \right\}$

$\beta^{-1} \sim$ “Transition time” \propto “Bubble size”

② ϕ/T dependence on (α, β)



Relic abundance of GWs

M. Kamionkowski, astro-ph/9310044 (PRD)

• Stochastic backgrounds of GWs:

$$\rho_{\text{GW}} = \frac{1}{32\pi G} \langle \dot{h}_{\alpha\beta} \dot{h}^{\alpha\beta} \rangle$$

↓ Wave eq. from Einstein eq. in weak field approximation $\left(-\square \left(h_{\mu\nu} - \frac{1}{2} \eta_{\mu\nu} h^\alpha{}_\alpha \right) = 16\pi G T_{\mu\nu} \right)$

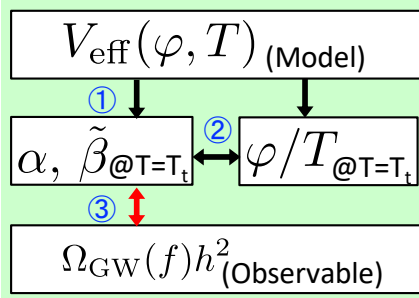
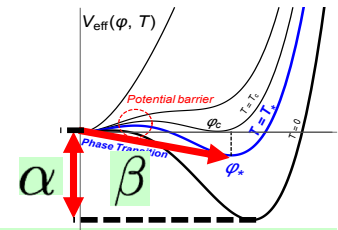
$$\sim \frac{8\pi G \rho_{\text{kin}}^2}{\beta^2}$$

$$\Omega_{\text{GW}} = \frac{\rho_{\text{GW}}}{\rho_{\text{tot}}} \simeq \left(\frac{H}{\beta} \right)^2 \left(\frac{\kappa \alpha}{1 + \alpha} \right)^2 = \tilde{\beta}^{-2} \sim (H \langle R \rangle)^2$$

$$\rho_{\text{tot}} (= \frac{\rho_{\text{vac}}}{(=\epsilon)} + \rho_{\text{rad}}) = \frac{3H^2}{8\pi G}$$

$$\alpha = \frac{\rho_{\text{vac}}}{\rho_{\text{rad}}} \quad \kappa = \frac{\rho_{\text{kin}}}{\rho_{\text{vac}}}: \text{Efficiency factor}$$

GWs from 1stOPT

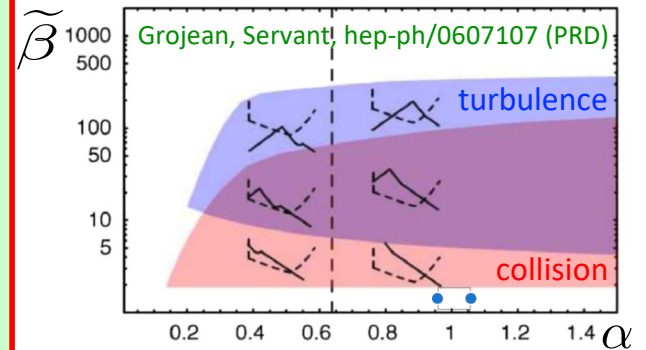


~ Probing the Higgs potential by GW observations ~

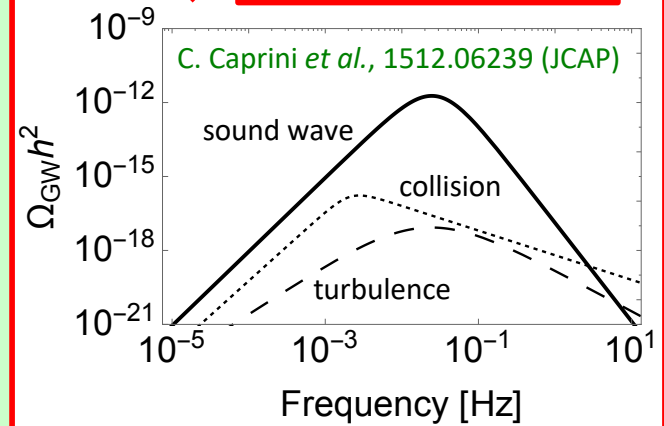
Characteristic parameters of 1stOPT

- α is defined as $\alpha \equiv \frac{\epsilon}{\rho_{\text{rad}}}\bigg|_{T=T_t}$. (ρ_{rad} is energy density of rad.)
 - Latent heat: $\epsilon(T) \equiv -\Delta V_{\text{eff}}(\varphi_B(T), T) + T \frac{\partial \Delta V_{\text{eff}}(\varphi_B(T))}{\partial T}$
 - $\alpha \sim$ "Normalized difference of the potential minima"
- β is defined as $\beta \equiv \frac{1}{\Gamma} \frac{d\Gamma}{dt}\bigg|_{t=t_t} \rightarrow \tilde{\beta} \left(\equiv \frac{\beta}{H_t} \right) = T_t \frac{d(S_3(T)/T)}{dT}\bigg|_{T=T_t}$
 - Bubble nucleation rate: $\Gamma(T) \simeq T^4 e^{-\frac{S_3(T)}{T}}$
 - 3-dim. Euclidean action: $S_3(T) = \int dr^3 \left\{ \frac{1}{2} (\vec{\nabla}\varphi)^2 + V_{\text{eff}}(\varphi, T) \right\}$
 - $\beta^{-1} \sim$ "Transition time" \propto "Bubble size"

③ $\Omega_{\text{GW}} h^2(f)$ as a function of (α, β)



$(\alpha \uparrow, \beta \downarrow) \Rightarrow \Omega_{\text{GW}} h^2 \uparrow$



Relic abundance of GWs $\Omega_{\text{GW}} \propto \left(\frac{H}{\beta}\right)^n \left(\frac{\kappa\alpha}{1+\alpha}\right)^m$

- "Sound waves" (Compressional plasma) [$n=1, m=2$]
- "Bubble collision" (Envelope approximation) [$n=2, m=2$]
- "Magnetohydrodynamic turbulence in the plasma" [$n=2, m=3/2$]

→ Exact formulae based on the numerical simulation are shown in C. Caprini *et al.*, 1512.06239 (JCAP)

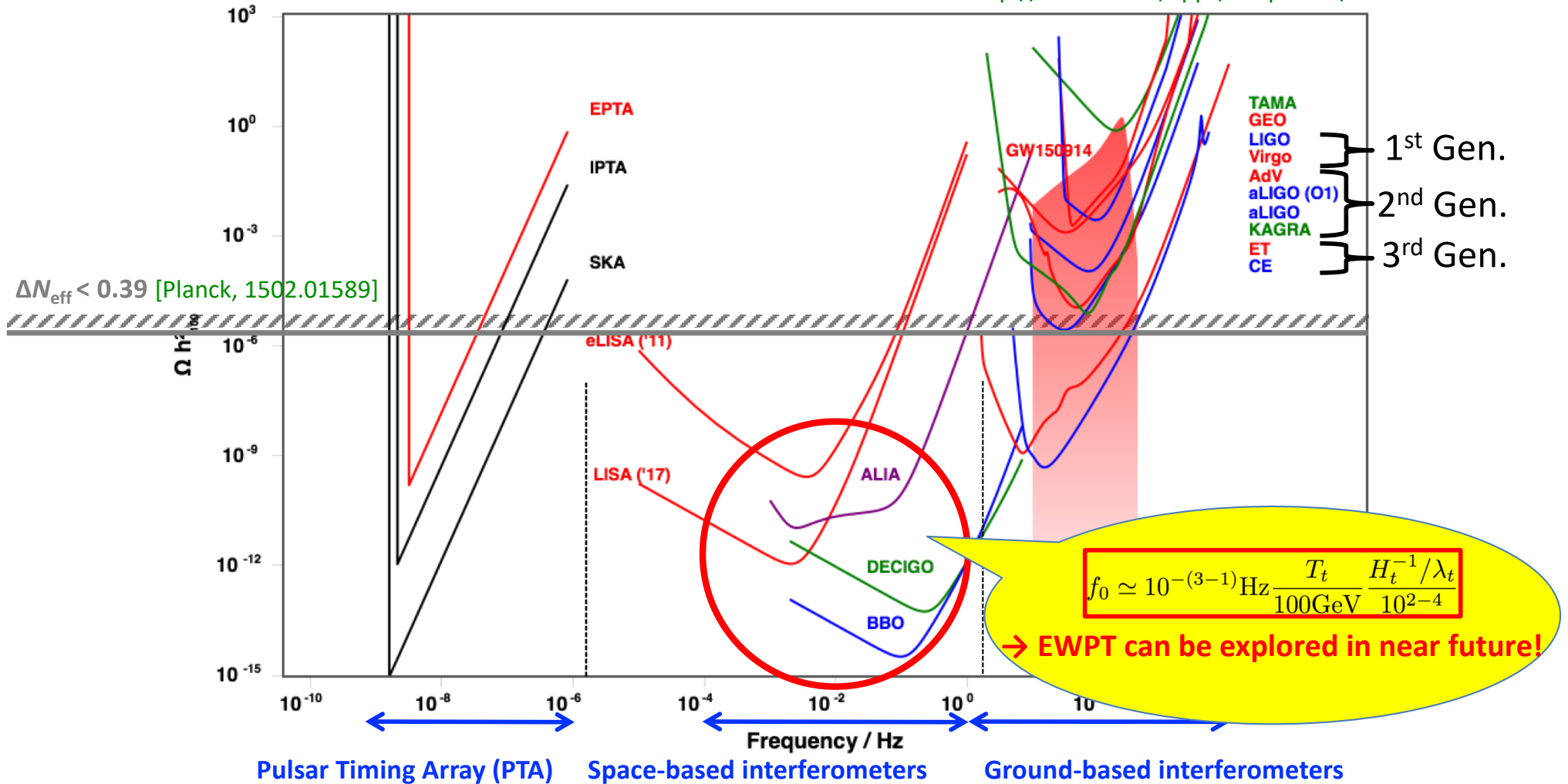
Red shifted frequency $f_0 = \frac{a_t}{a_0} f_t$ t : transition scale @EW (~100GeV) $f_0 \simeq \frac{10^{-(3-1)} \text{Hz}}{100 \text{GeV}} \frac{T_t}{10^2-4} \frac{H_t^{-1}/\lambda_t}{10^{2-4}}$ ($H_t^{-1}/\lambda_t \propto \tilde{\beta}$)

$f_t \simeq 10^9 \text{Hz}$

Target frequency for LISA/DECIGO

Sensitivity of GW detectors

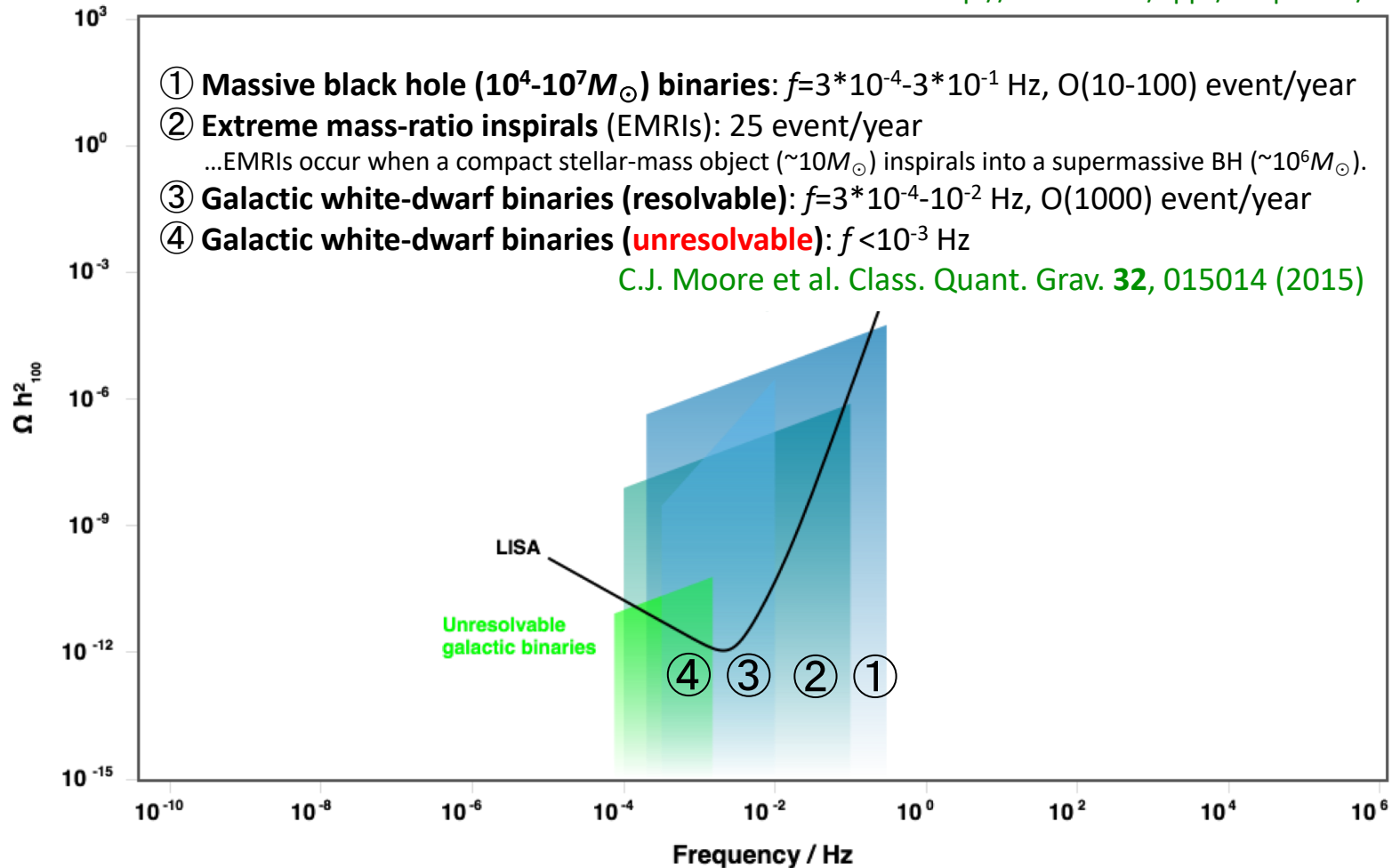
<http://rhcole.com/apps/GWplotter/>

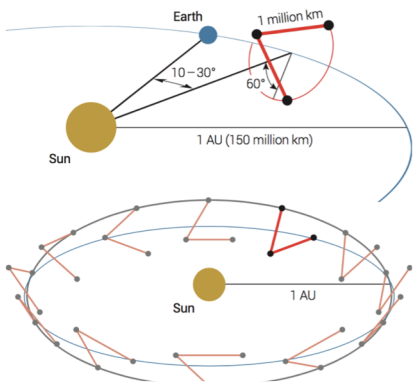


$L=O(10^6)\text{km}$ (LISA), 1000km (DECIGO), 4km (LIGO), 3km (Virgo, KAGRA)

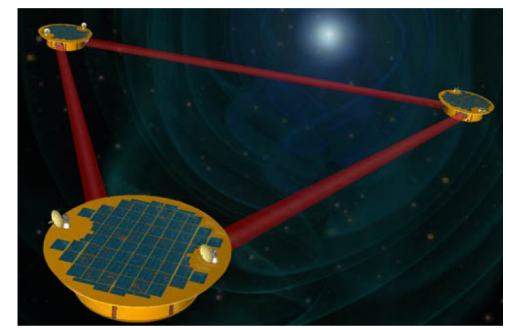
Foreground noise

<http://rhcole.com/apps/GWplotter/>

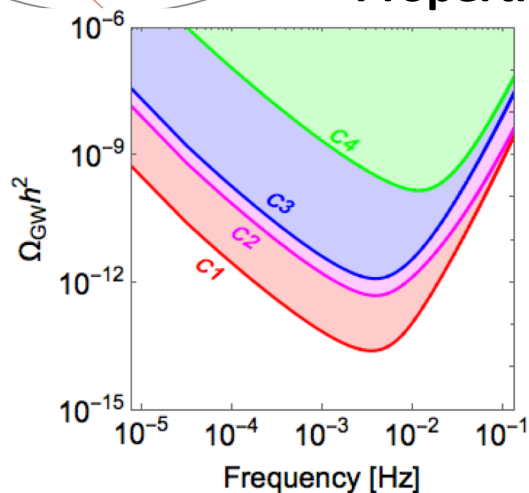




LISA design decided



Properties of the representative eLISA configurations



Name	C1	C2	C3	C4
Full name	N2A5M5L6	N2A1M5L6	N2A2M5L4	N1A1M2L4
# links	6	6	4	4
Arm length [km]	5M	1M	2M	1M
Duration [years]	5	5	5	2
Noise level	N2	N2	N2	N1

C1 : old LISA configuration

[eLISA cosmology WG report, arXiv:1512.06239 (JCAP)]

(*) The signal-to-noise ratio (SNR) = 1 is taken to assess the detectability of the GW signal.

$$SNR = \sqrt{\mathcal{T} \int_{f_{min}}^{f_{max}} df \left[\frac{h^2 \Omega_{GW}(f)}{h^2 \Omega_{Sens}(f)} \right]^2}$$

- **Number of laser links: 6** [corresponding to 3 interferometer arms] → Determined at eLISA symposium [Sept. 2016, U. of Zurich]
 - **Arm length: 2 - 5** million km
 - **Duration: 3 - 10** years data taking
 - **Noise level: N2** (expected) [10 times larger than N1 (required)] → Determined by receiving LISA pathfinder result [PRL116, 231101 (2016)]
- } Extra budget was estimated

ESA approval: **June, 2017**; Launch: **2034**

DECI-hertz Interferometer Gravitational Wave Observatory (DECIGO)

“DECIGO correlation with four clusters”:

DECIGO will be delivered into heliocentric orbits with two clusters nearly at the same position and the other two at separate positions

